Biophysical Journal Volume 105 November 2013 2024–2035

Intensity Correlation-Based Calibration of FRET

László Bene,[†*] Tamás Ungvári,[‡] Roland Fedor,[†] László Sasi Szabó,[†] and László Damjanovich[†]
[†]Department of Surgery and [‡]Department of Biophysics and Cell Biology, Medical and Health Science Centre, Faculty of Medicine, University of Debrecen, Debrecen, Hungary

ABSTRACT Dual-laser flow cytometric resonance energy transfer (FCET) is a statistically efficient and accurate way of determining proximity relationships for molecules of cells even under living conditions. In the framework of this algorithm, absolute fluorescence resonance energy transfer (FRET) efficiency is determined by the simultaneous measurement of donor-quenching and sensitized emission. A crucial point is the determination of the scaling factor α responsible for balancing the different sensitivities of the donor and acceptor signal channels. The determination of α is not simple, requiring preparation of special samples that are generally different from a double-labeled FRET sample, or by the use of sophisticated statistical estimation (least-squares) procedures. We present an alternative, free-from-spectral-constants approach for the determination of α and the absolute FRET efficiency, by an extension of the presented framework of the FCET algorithm with an analysis of the second moments (variances and covariances) of the detected intensity distributions. A quadratic equation for α is formulated with the intensity fluctuations, which is proved sufficiently robust to give accurate α-values on a cell-by-cell basis in a wide system of conditions using the same double-labeled sample from which the FRET efficiency itself is determined. This seemingly new approach is illustrated by FRET measurements between epitopes of the MHCI receptor on the cell surface of two cell lines, FT and LS174T. The figures show that whereas the common way of α determination fails at large dye-per-protein labeling ratios of mAbs, this presented-as-new approach has sufficient ability to give accurate results. Although introduced in a flow cytometer, the new approach can also be straightforwardly used with fluorescence microscopes.

INTRODUCTION

Fluorescence resonance energy transfer (FRET) is a powerful and popular method for the determination of proximities between suitable fluorophores, called donors and acceptors, in the 1–10-nm distance range (1). In addition to its ability to perform fluorescence lifetime-based measurements, several steady-state realizations already exist—for example, for measuring simple donor quenching, acceptor sensitization, donor photobleaching, acceptor photobleaching, donor anisotropy, and acceptor anisotropy (2–6). Amongst these uses, the dual-laser flow cytometric resonance energy transfer (FCET) method (7,8) has proven itself unique—such uniqueness due not only to its high statistical power, but also to its relative simplicity, merely requiring the use of flow cytometer types that are already commercially available. (For flow cytometric applications of FRET, see Szöllősi et al. (9).)

The essence of FCET is that, in addition to the parameters proportional to the donor and acceptor concentrations, FRET efficiency is determined as a common value for both quenching efficiency and the percent-enhancement of sensitized emission after correction for the difference in signal detectabilities in the donor and acceptor channels with a scaling factor called α (7,8,10). This factor—which we call from now on "spectral α," referring to its way of determination—is generally determined from the mean intensities of the samples labeled with donor and acceptor only in the knowledge of the amounts of the donor and acceptor dyes (which are proportional to the dye-per-protein labeling ratios of the dye-targeting ligands and the number of receptors labeled by the ligands) and from the relative absorption coefficient of the donor and acceptor measured at the donor's excitation wavelength.

For the spectroscopic determination of α, two different epitopes on the same receptor are targeted by the donor- and acceptor-tagged ligands, and the same receptor epitope is labeled either with the donor-stained or the acceptor-stained ligand, where in both cases the 1:1 stoichiometry guaranties the required equal receptor numbers condition for the determination of the spectral α. Trouble arises when the relative numbers of the donor- and acceptor-tagged receptors are not known, e.g., in the case of engineered visible fluorescent proteins (VFPs), although sometimes a 1:1 stoichiometry can be guaranteed here (11,12). In rare cases of this kind when the donor-acceptor spatial topology is rather well described—e.g., in a Stryer-Haugland type of an experiment with rigid amino-acid polymers as donor-acceptor spacers (1,9,10), or its recently refined versions using DNA construct-based rulers, where the orientation factor (κ^2) is more accurately defined (13,14)—a way out is offered by the known values of FRET efficiency estimated from the known donor-acceptor separation distances: In this inverse problem, the system of FCET equations (see Eqs. S1–S3 in the Supporting Material) is solved for α in the knowledge of FRET efficiency.

In a somewhat more complicated statistical approach restricted by the condition of constant donor-acceptor

Submitted August 27, 2013, and accepted for publication September 26, 2013.

*Correspondence: bene@med.unideb.hu

Editor: Amitabha Chattopadhyay.

0006-3495/13/11/2024/12 $2.00

http://dx.doi.org/10.1016/j.bpj.2013.09.041

concentration ratio, least-squares estimation can also be used (10). Here FRET efficiency is estimated in two ways:

1. As defined by α via the system of equations for FCET (see Eqs. S1–S3 in the Supporting Material) and
2. From one extra equation when the sensitized emission intensity is expressed with the acceptor-donor absorbance ratio instead of α—and the difference of estimations is minimized.

In this communication, we develop what we believe to be a new approach for the determination of α based on a characteristic of intensity distributions, the width of the detected distributions, and the covariances between the intensity distributions. Here the width represents the standard deviation, defined as the square-root of variance (second central moment), which is an average of the squares of the deviations from the mean, i.e., the mean-squared fluctuation around the mean. Covariance is analogously defined between two different intensities: as average products, of fluctuations of two different intensities, around the respective means (15,16). We hypothesize that similarly to the distribution means, distribution variances and covariances as well as the corresponding fluctuation products convey information on the processes behind the intensity distributions. This is also corroborated by the fact that in a broad family of distributions, the distribution mean is not independent from the corresponding distribution variance (e.g., Poisson, log-normal, and Weibull distributions) (17). In the context of α determination, our hypothesis means that the difference in detection sensitivities of the donor and acceptor signals should also be manifested in differences in the widths and covariances of the donor- and acceptor-related fluorescence intensity distributions.

For an overview of the organization of the article, please see the Supporting Material.

For a Glossary of Terms, see the Appendix.

MATERIALS AND METHODS

Information on cells, specificity of monoclonal antibodies, fluorescent staining of monoclonal antibodies (mAbs), and labeling of cells with fluorescent ligands is found in the Supporting Material.

Flow cytometric energy transfer measurements

FRET efficiency was determined in a combined manner from the donor quenching and the sensitized emission of acceptor (7,8) on a cell-by-cell basis. For measuring FRET applying both the Alexa-Fluor 488-546 and Alexa-Fluor 546-647 (or Cy5) donor-acceptor dye-pairs (18), we used the FACSVantage SE flow cytometer with a FACSDiVa extension (Becton-Dickinson, Franklin Lakes, NJ), equipped with triple-laser excitation, and with the lasers operating in the single-line mode at 488 nm (Coherent Enterprise Ar^+-ion gas laser; Innova Technology, Coherent, Santa Clara, CA), at 532 nm (a diode-pumped solid-state laser), and at 632 nm (model No. 127 He-Ne gas laser; Spectra Physics, Santa Clara, CA).

In addition to the forward-angle light-scattering (FSC) signal, the following four signals were collected for each cell running through the laser beams with the transmitted wavelength range and the specifications of the realizing band path filters in parentheses (all filters from A. F. Analysentechnik, Tübingen, Germany): 1), the right angle (or perpendicular) side-scattered light (SSC) signal at the 488/532-nm laser line (BP 488/10, BP 532/10 filters) to separate debris and cells based on size and intracellular morphology in FSC-SSC dot-plots; 2), the donor (Alexa-Fluor 488 or 546) and 3), the acceptor (Alexa-Fluor 546 or 647) signals I_1 (quenched donor intensity) and I_2 (containing sensitized emission), both excited at the 488/532-nm wavelength, the maximum of the donor absorption and detected through a DM 561 LP/DM 630 LP dichroic mirror in the 515–545 nm (DF 530/30 BP filter)/570–620 nm (DF 595/50 BP filter); and 4), the 570–620 nm (DF 595/50 BP filter) >635 nm (DF 635 LP filter) wavelength ranges.

The FRET problem has three unknowns (FRET efficiency, and the donor and acceptor concentrations) for the determination of which, in addition to the aforementioned I_1 and I_2 signals, a third fluorescence intensity I_3 is also necessary (7,8): the acceptor intensity excited at 532/632 nm, close to the maximum of the acceptor absorption, and also detected in the >561 nm (DF 561 LP filter) >635 nm (DF 635 LP filter) wavelength range. With the above I_1, I_2, and I_3 signals, the A', d', d_0, p, q, α and the FRET indices Q, E_0, and E are calculated as described in Theoretical Results. These parameters were determined on a cell-by-cell basis in the gated cell population with a home-made software program called REFLEX (http://www.biophys.dote.hu/research.htm, http://www.freewebs.com/cytoflex.htm), specialized for processing flow cytometric histograms (19) to be displayed as frequency distribution curves (Fig. 2). A case study of the FCET calculation is presented in the Supporting Material. The frequency distribution of the α-factor shown in Fig. 2 has been computed with the software MATLAB, Ver. 7.0.1 (The MathWorks, Natick, MA).

A case study of the FCET calculation, as well as technical details of fluorescence lifetime measurement by fluorescence lifetime imaging microscopy (FLIM), is presented in the Supporting Material.

THEORETICAL RESULTS

Introducing the α-factor

The α-factor plays a crucial role in the determination of FRET efficiency in the FCET measuring scheme. Formally, according to the theory of FCET detailed in the Supporting Material, the E FRET efficiency is computed from the primarily measured A' quantity via a kind of normalization of A' by α as expressed by the relationship

$$E = A'/(\alpha + A'),$$

which is analogous to Förster's $E = R_0^6/(R^6 + R_0^6)$. Phenomenologically, it is a conversion or normalization factor between the donor's and acceptor's emission channels (meaning the acceptor signal in the acceptor channel corresponding to the signal of a single donor molecule in the donor channel). Its value is the product of the ratio of equipment sensitivities of the two channels, η_a/η_d (dictated by optical collection angles of detectors, photomultiplier sensitivities, and gains of electronic amplifiers and photomultiplier voltages) and the ratio of the quantum efficiencies, Y_a/Y_d of the donor and acceptor fluorophores on the labels

$$\alpha = \frac{\eta_a}{\eta_d} \cdot \frac{Y_a}{Y_d}. \quad (1)$$

If the cell surface concentration ratio of the targeted receptors (binding sites), B_a/B_d, is known, α can be determined from the mean fluorescence intensities M_a and M_d of the samples labeled with only acceptor and donor, respectively, with the molar decadic absorption coefficients of the donor and acceptor ε_d and ε_a (both in M^{-1} cm^{-1}) and the dye-per-protein labeling ratios of the dye-targeting ligands L_d and L_a (spectroscopic α):

$$\alpha = \frac{\varepsilon_d}{\varepsilon_a} \cdot \frac{L_d}{L_a} \cdot \frac{B_d}{B_a} \cdot \frac{M_a}{M_d}. \quad (2)$$

The form of Eq. 2 for α is based on the assumption that fluorescence intensity is a linear function of the dye concentration. This may not be fulfilled at large dye local concentrations, e.g., when several dye molecules are closely packed on a carrier ligand.

Determination of α with intensity correlations

The determination of α via Eq. 2 is problematic for the following reasons:

1. The ratio of the labeled binding sites B_d/B_a is generally not known; it is considered an unknown parameter of the FRET problem. In our practice, α is mostly determined by using the same type of ligand conjugated with the donor and acceptor fluorophores. Alternatively, two different ligands are used, which bind to two different binding sites on the same receptor, e.g., donor-conjugated L368 and acceptor-conjugated W6/32 mAbs binding to the β_2-microglobulin (β_2m) and heavy-chain subunits of the major histocompatibility complex class I (MHCI) receptor, when $B_d/B_a = 1$. However, in important cases of genetically engineered light-emitting proteins, the ratio of the number of labeled receptor sites may be inherently not known, and Eq. 2 cannot be applied directly, in a straightforward manner (10).
2. Even if the ratio of the labeled binding sites is known, the application of Eq. 2 can lead to errors in α introduced by the labeling ratio-dependence of light emission of the fluorophore-conjugated labels (mAbs) and/or the labeling-ratio dependence of binding of the ligands to their receptors. As to the light emission, by increasing labeling ratios, it decreases on average due to the larger formation probabilities of dim complexes (efficient traps of excitation energy conveyed by homo-FRET), meaning that the true number of emitters (i.e., the effective labeling ratio) is smaller than the nominal one (20–24).

The above problems with the determination of α inspired us to find more efficient and robust ways of determination of α resistant to the changes of the effective labeling ratios (effective quantum efficiency) that do not require the prior knowledge of the receptor numbers. A way forward is offered by fluctuation analysis of the measured cell-by-cell fluorescence distributions in the form of calculated variances and covariances (also called second moments) and their possible dependence on the respective mean values (fluorescence intensities and other quantities).

By computing the variance of the I_1 donor signal, a quadratic equation for α can be set up that is resistant enough to experimental uncertainties for giving a meaningful α-value as its positive root in most of the cases. Starting out from Eq. S1 in the Supporting Material, the variance of I_1 can be written as

$$(I_1, I_1) = (I_d, I_d) + (I_d \cdot E, I_d \cdot E) - 2 \cdot (I_d, I_d \cdot E), \quad (3)$$

where symbol (ξ,ψ) designates the covariance of quantity ξ with ψ (as random variables), defined as according to (25)

$$(\xi, \psi) = \sum_{i=1}^{n} \left(\xi_i - \overline{\xi}\right) \cdot \left(\psi_i - \overline{\psi}\right)/n, \quad (4)$$

where n is the number of cells (or pixels in the case of imaging).

After replacing I_d and $I_d \times E$ in Eq. 3 with

$$I_d = I_1 \cdot \left(1 + A'/\alpha\right) \quad (5)$$

and

$$I_d \cdot E = I_1 \cdot A'/\alpha \quad (6)$$

obtainable from Eqs. S12 and S13 in the Supporting Material, and by introducing the designations

$$d = (I_d, I_d) \quad (7)$$

and

$$d' = (I_1, I_1) \quad (8)$$

for the second moment of the donor intensity unperturbed by FRET (but possibly perturbed by steric interactions) and for the donor intensity perturbed by both FRET and possible steric interactions, respectively, we obtain the following quadratic equation for α:

$$D \cdot \alpha^2 - 2 \cdot p \cdot \alpha - q = 0, \quad (9)$$

with the shorthand notations

$$D = d - d', \quad (10)$$

$$p = \left(I_1, I_1 \cdot A'\right), \quad (11)$$

$$q = \left(I_1 \cdot A', I_1 \cdot A'\right). \quad (12)$$

An alternative deduction of Eq. 9 is presented in Eq. S27 in the Supporting Material. For a summary of the correlation method, please see Fig. 1.

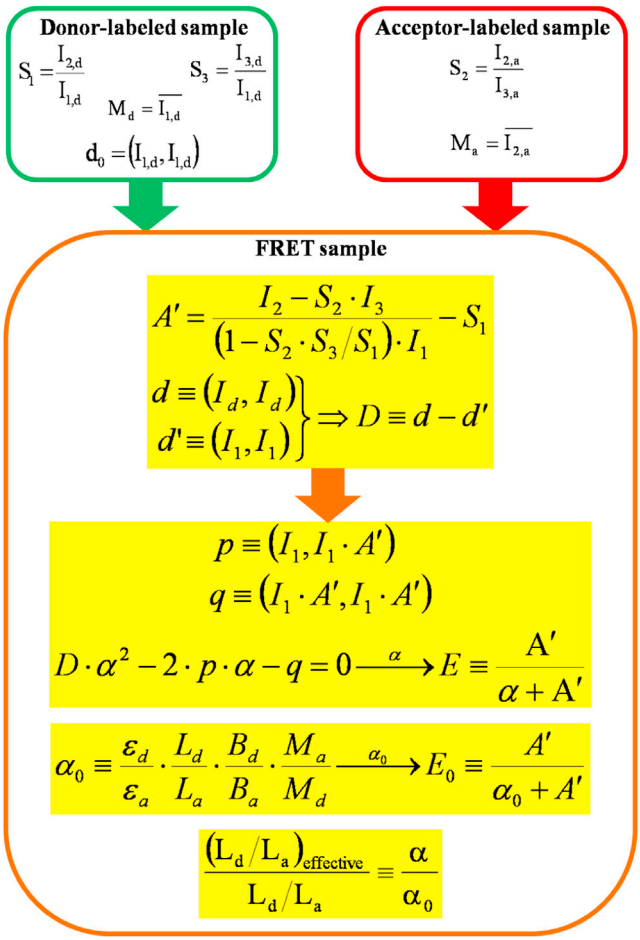

FIGURE 1 Flow-chart and summary of the main formulae for determining FRET based on intensity correlations. As the starting point, single donor-only labeled samples are analyzed for determining the S_1, S_3 spectral spillage factors, the M_d intensity mean, and the d_0 intensity variance, then single acceptor-labeled samples are analyzed for determining the S_2 spectral spillage factor and the M_a intensity mean. In the knowledge of S_1, S_2, and S_3, the FRET-related quantity A' is determined based on the double-labeled FRET sample: A' is a single-valued, monotonously increasing function of the transfer efficiency E for the accurate calculation of which a scaling of A' with the scaling factor α is necessary. After scaling of A' with α, FRET efficiency E is calculated as $E = A'/(\alpha + A')$, with the meaning $A'/\alpha = (R_0/R)^6$ (from Förster's formula). Calculation of covariance-based α begins with determination of D, the difference between the variance of the hypothetical (immeasurable, indirectly determined) donor intensity when FRET is switched off (d), and the variance of donor intensity (measurable) when FRET is switched on (d'), both characterizing the double-labeled FRET sample. In the absence of any steric interaction between the dye-targeting labels (e.g., no competition) instead of d, the d_0 variance of the donor-only sample can be used for calculation of D. In the presence of steric influence, the functional dependence of the change in the intensity variance (Q') on the change in mean intensity (Q) characterized with the m slope and b intercept parameters ($Q' = m \cdot Q + b$) can be used for estimating d and D on the FRET sample in the knowledge of d', A', and α. It can be noted that whereas in the former case D does not depend on α, in the latter case it does, with the consequence that a cubic equation should be used for α, instead of a quadratic one (see below). After determining D (or expressing it as the function of α), coefficients of p and q are calculated with I_1, and A' on the double-labeled sample. In the knowledge of D, p, and q, a quadratic (or more complicated, depending on the nature of D, see also the Supporting Material) equation is solved for α. The fact that the D, p, and q coefficients are population averages of fluctuation (deviation from the mean) products implies two alternatives for solution of the equation for α: either it can be solved for α for each individual cell, i.e., on a cell-by-cell basis and histograms of α are created from which some characteristic expressing average behavior (mean, mode, median) is calculated (followed when D is independent of α); or the averages of the appropriate fluctuation product histograms (cell-by-cell distributions of D, p, q) are calculated first, then the equation is solved for an average α (followed when D depends on α). Finally, E is calculated with α and A' on a cell-by-cell basis. The α-factor in the conventional way is determined from the relative absorption, labeling ratio, receptor number, and intensity (spectral α or α_0). FRET efficiency of E_0 is calculated with α_0 and A' on a cell-by-cell basis. By taking a ratio, $\alpha/\alpha_0 = (L_d/L_a)_{effective}$ can be introduced, expressing the reduction in quantum yield or binding efficiency of the fluorescently labeled ligand as the function of the degree of labeling of ligands.

As to the meaning of the quantities D, p, and q in Eq. 9: D is the reduction of variance of the donor intensity due to FRET expressing increasing information content (or decreasing entropy) of the donor signal, q is the information (or entropy) conveyed by FRET from the donor channel toward the acceptor channel (26), and p is the covariance between transferred energy and remaining energy at the donor's site representing possible dependence of FRET on the donor's concentration (which could occur for nonrandom receptor distributions (27)).

More explicitly, by using Eq. S10 in the Supporting Material for A', the p and q parameters can be expanded in zero-, first-, and second-order terms of the S_1, S_2, and S_3 spillage factors—which are generally smaller than unity—multiplied with the covariances and variances of the basic I_1, I_2, and I_3 intensities:

$$p = \frac{(I_1, I_2) - S_2 \bullet (I_3, I_3)}{1 - S_2 \bullet S_3/S_1} - S_1 \bullet (I_1, I_1), \qquad (13)$$

and

$$q = \frac{(I_2, I_2) - 2 \bullet S_2 \bullet (I_2, I_3) + S_2^2 \bullet (I_3, I_3)}{(1 - S_2 \bullet S_3/S_1)^2} - \frac{2 \bullet S_1 \bullet [(I_1, I_2) - S_2 \bullet (I_1, I_3)]}{1 - S_2 \bullet S_3/S_1} + S_1^2 \bullet (I_1, I_1). \qquad (14)$$

By replacing the spillage factors with zero, Eqs. 13 and 14 inform us that whereas p essentially reflects the covariance of the quenched donor fluorescence with the sensitized acceptor fluorescence ($p = (I_1, I_2)$), q reflects the variance of the sensitized acceptor fluorescence ($q = (I_2, I_2)$).

Applications of the variance equation for α (Eq. 9)

The case of sterically noninteracting donors and acceptors

For the application of Eq. 9, the spectral spillage factors S_1, S_2, and S_3 are determined from the I_1, I_2, and I_3 intensities

of the single donor- and acceptor-stained samples, and the parameter A' is calculated with the spillage factors and the intensities of the double-labeled sample. Then from A' and I_1, the covariance p and variance q terms (the second-order moments) are calculated. The most problematic factor in Eq. 9 is D: although d' is calculated from I_1 as its variance, d, the variance of I_d is unknown due to a lack of a prior knowledge on the distribution of unperturbed donor intensity in the presence of the acceptor-carrying ligand. Nevertheless, some work-around can be found: With the application of an unlabeled (dim) version of the ligands used for targeting the acceptor, possible influences of the presence of the acceptor-carrying ligands can be revealed, and the variance of the detected I_1 intensity can be used as an estimation of d in Eq. 10. In the absence of steric interactions, the d value can also be estimated with the variance d_0 of I_1 measured on the donor-only sample.

Lower and upper limits for α

A generally applicable inequality can also be stated, based on the fact that FRET reduces the value of d, i.e., $d' < d$,

$$0 \le D \le d \le d_0, \tag{15}$$

where the value of D is zero when $E = 0$ ($d = d'$), and $D = d$ when $E = 100\%$ ($d' = 0$), and because $d < d_0$ can be generally assumed (where d_0 is the variance of I_1 of the donor-only sample, i.e., $d_0 = (I_1,\ I_1)_{\text{donor only}}$). Based on the chain of inequalities in Eq. 15, lower and upper limits for α—defined by the conditions $D = d_0$ and $D = 0$, respectively—can always be computed.

Approaches when d is unknown: estimation of d from d′ and A′ based on the variation of d with the mean intensity

1. For the recording of $Q'-Q$ plots, the first approach is based on the experience that the variance of the I_1 signal shows a monotonic dependence on the mean of I_1 intensity, which can be taken as linear with a good approximation (as judged from correlation coefficients $R^2 > 80\%$, see also Fig. 3 *A*). Equivalently, from this statement it also follows that if a relative change Q' is defined with the donor-moments in the absence and presence of FRET (generally the sum of quenching induced by FRET and the effects of possible steric interactions, as a kind of FRET index), Q' should also linearly depend on the relative change Q in intensity means. This circumstance implies that if a relationship between Q' and Q can be stated, then the validity of this relationship in the presence of acceptor-bearing ligands could be used for the estimation of the unknown value of d. Detailing now the procedure: If Q (intensity quenching) is defined as

$$Q = 1 - I_1/I_{d,0}, \tag{16}$$

where I_1 and $I_{d,0}$ are donor intensities in the presence and absence of acceptor-bearing ligands (mAbs), and if Q' (i.e., quenching of variance) is defined as

$$Q' = 1 - d'/d_0 \tag{17}$$

with the corresponding donor-moments, then a linear dependence of Q' on Q can also be expected, with a slope (i.e., amplification) m and intercept (i.e., zero-offset) b. These constants can be experimentally determined in the optical conditions of the FRET measurement (see also Eq. 27):

$$Q' = m \cdot Q + b. \tag{18}$$

For determining the m and b constants in Eq. 18, the donor intensity and its variance may be changed also by processes—i.e., quenching processes and steric interactions—other than FRET, inasmuch as the coefficients remain resistant to the exact type of the intensity-perturbing process in constant optical conditions. The requirement is that the biological contribution to the total variance should be the same as in the studied FRET process. Variation of donor intensity may be accomplished by changing the amount of the acceptor—e.g., via changing the labeling ratio of the acceptor-stained ligand, or the expression levels of receptors targeted by the acceptor with IFNγ, as in this study, or KI quenching (28). The advantage of formulating the dependence of d on the mean intensity via the dependence of Q' on Q is that the latter is scale-invariant.

For the estimation of d via Eq. 18 with the measured values of d' and A', d' is expressed first from Eq. 17 as the function of Q', into which the value of Q', as expressed with Q according to Eq. 18, is plugged. Finally, Q is expressed with A' and α according to Eq. S12 in the Supporting Material, if E is replaced by Q. The result is the following expression of d as the function of A' and α:

$$d = \frac{d'}{1 - m \cdot A'/(\alpha + A') - b}. \tag{19}$$

After plugging this estimation of d into Eq. 10, Eq. 9, originally quadratic in α, is converted into an equation now cubic in α,

$$p_3 \cdot \alpha^3 + p_2 \cdot \alpha^2 + p_1 \cdot \alpha + p_0 = 0, \tag{20}$$

with coefficients

$$p_3 = b \cdot d', \tag{21}$$

$$p_2 = (m + b) \cdot A' \cdot d' - 2 \cdot (1 - b) \cdot p, \tag{22}$$

$$p_1 = -2 \cdot (1 - m - b) \cdot A' \cdot p - (1 - b) \cdot q, \tag{23}$$

$$p_0 = -(1 - m - b) \cdot A' \cdot q. \quad (24)$$

The acceptable solution of Eq. 20 (real, positive, and large enough for producing $E < 1$) is designated with α_{cubic} in Table 1 and Table S1 in the Supporting Material. By inspecting Eqs. 20–24, it can be seen that the presence of a zero-offset ($b \neq 0$) gives rise to the third power in Eq. 20, otherwise (with $b = 0$) Eq. 20 turns into a quadratic equation.

2. Estimating intensity variation of d from a single cell-by-cell distribution of the I_1 donor intensity is done by successive gating on a second parameter (see Eq. S14 in the Supporting Material).
3. Estimating d by using Eq. 2, a hybrid approach, is done when the labeling ratios are small (see Eq. S23 in the Supporting Material) and linearity is guaranteed.

EXPERIMENTAL RESULTS

Comparative measurements of FRET between epitopes of MHCI at different labeling ratios of mAbs on the surface of FT T-lymphoblast cells: I. Alexa-Fluor 546-647 dye pair

Table 1 reports on FRET measurements between Alexa-Fluor 546- and Alexa-Fluor 647-conjugated mAbs bound to epitopes of MHCI. Intramolecular proximity is monitored when two different mAbs are used against the two subunits of MHCI: L368 against the light chain ($\beta_2 m$) and W6/32 against the heavy chain conjugated with the donor and acceptor, respectively, in the forward direction (L368 → W6/32, Table 1 *A*), and, vice versa, in the reverse direction (W6/32 → L368, Table 1 *B*). Approximately equal and large FRET efficiencies are expected in these cases, based on the rather well-defined distance of these subunits of ~7.7 nm

TABLE 1 Conventional and the covariance-based α-factors

FRET pairs						α-factors			FRET efficiencies (%)		
Donor: Alexa-Fluor 546		Acceptor: Alexa-Fluor 647		Labeling ratio		Spectral	Covariance-based		Quenching	Quenching and sensitized emission	
mAb	Epitope	mAb	Epitope	L_d	L_a	α_0[a]	α[b]	α_{cubic}[c]	Q[d]	E_0[e]	E[f]
A											
L368	β_2m	W6/32	MHCI	4.7	1.7	10.07	0.35	—	28	2	30
L368		W6/32 low[g]	heavy-chain			9.78	0.40	—	19	2	21
L368 low[g]		W6/32				9.88	0.29	—	26	1	26
B											
W6/32	MHCI	L368	β_2m	1.5	2.1	0.13	0.14	—	19	26	25
W6/32	heavy-chain	L368 low[g]				0.12	0.09	—	16	18	22
W6/32 low[g]		L368				0.13	0.16	—	23	27	24
C											
L368	β_2m	L368	β_2m	4.7	2.1	3.96	0.16	0.21	39	1	13[h]
W6/32	MHCI	W6/32	MHCI	1.5	1.7	0.33	0.10	0.14	40	6	11[h]
	heavy-chain		heavy-chain								

Deduced FRET efficiencies measured between the β_2m (light-chain) and heavy-chain subunits of the MHCI receptor as well as between its heavy-chain subunits on the surface of FT T-lymphoblast cells by using Alexa-Fluor 546- and Alexa-Fluor 647-conjugated mAbs.

[a]The conventional (or spectral) α-factors (α_0) have been calculated according to Eq. 2 of the main text by using the mean intensities of the samples labeled with the donor and the acceptor as well as the labeling ratios and absorption coefficients. Because of the 1:1 stoichiometry of the two subunits of the same MHCI molecule, unity was used for the ratio of the labeled receptors (B_d/B_a). All data in this table are representative ones of three different measurements giving similar results, with relative errors <15% (mean ± SE).

[b]Covariance-based α-factor at the donor side (α) was determined as the mean value of the corresponding cell-by-cell distribution of α obtained as the positive root of the quadratic polynomial in Eq. 9 written for the cell-by-cell distributions of the D, p, and q coefficients, examples of which are shown in Fig. 2. In calculation of the D coefficient in Eq. 9, for the noncompeting case of FRET measurement between the β_2m and heavy-chain subunits, the d value of the FRET sample was approximated by the mean of d_0 distribution of the corresponding single-donor labeled sample.

[c]In the case of FRET indicating homo-association between the MHCI receptors, instead of using d_0 of the single-donor labeled sample, the d' value of the FRET sample has been corrected according to Eq. 19 and the positive root of the cubic polynomial in Eq. 20. This resulted in a meaningful FRET efficiency (α_{cubic}) that was used in the calculation of E. Whereas the root of the quadratic polynomial of Eq. 9 has been found for each cell and the cell-by-cell distribution of α has been determined, this latter calculation have been carried out only with mean values.

[d]Quenching efficiency (Q) is defined as the relative change in the I_1 donor fluorescence due to the mAb used as acceptor. Mean values of the corresponding cell-by-cell distributions, defined as $Q = 1 - I_1/I_{1,d}$ where I_1 is intensity of the double-labeled sample and $I_{1,d}$ is the mean intensity of the sample labeled only with the donor, are listed. In the case of competing mAbs for the measurement of MHCI homo-association, it also contains the intensity-reducing effect of mAb competition and the effect of FRET.

[e]E_0 has been calculated as the mean of the corresponding cell-by-cell distribution obtained from the A' distribution by using $E_0 = A'/(\alpha_0 + A')$ (see Eq. S12 in the Supporting Material) with the conventional α-factor (α_0) as an input constant.

[f]E has been calculated as the mean of the corresponding cell-by-cell distribution obtained from the A' distribution by using $E = A'/(\alpha + A')$ with the covariance-based α-factor (α) as an input constant.

[g]In this case, "low" means one-half of the saturating amount of the mAb concentration. These values were calculated by using α_{cubic}, the solution of Eq. 20 with $m = 3.25$, $b = 0.17$ ($R^2 = 0.86$) obtained by fitting the corresponding Q–Q' plot like that shown in Fig. 3 *A*.

(29). In Table 1 *C*, the same epitope on the light or heavy chain is labeled by the donor- and acceptor-bearing mAbs of the same type (either L368 or W6/32), defining FRET pairs for measuring intermolecular proximities, i.e., homo-associations of the MHCI receptors. The quantities listed are chosen such a way as to enable comparison of α-factor and FRET indices obtained in the conventional way (spectral α or α_0, and Q, E_0) with those obtained with the believed-new method (covariance-based α-factors α, α_{cubic}, and E). Examples for the cell-by-cell distributions are shown on Fig. 2.

An important feature of the intramolecular FRET systems defined by the L368 and W6/32 mAbs is that because, in these cases, there is practically no steric interaction between these ligands, the simple donor quenching (Q) values themselves can serve as a kind of internal control for the E_0 and E FRET efficiencies determined with the α-factors (29,30). Whereas α_0 was calculated by using the labeling ratios listed, α was determined from the quadratic equation, the coefficients of which ($D = d - d'$, p, q) are defined by the appropriate variances and covariances determined from the donor- and double-labeled samples. Because in the intramolecular FRET case there is only a very small competition (<10%), the d moment of the FRET sample, which indicates variance of the hypothetical donor intensity when FRET would be switched off, can be replaced by the d_0 moment of the donor-only sample enabling calculation of D as $d_0 - d'$ instead of $d - d'$. This approximation would overestimate the real D and underestimate the real α in the case of significant competition between the donor- and acceptor-bearing ligands. The coefficient p is a covariance of I_1 and $I_1 \cdot A'$, and q is the covariance of $I_1 \cdot A'$ with itself (i.e., the variance), both determined on the same double-labeled FRET sample.

Regarding the calculation of α, the case of intermolecular FRET describing homo-associations is quite different. In this case, there is an inherent steric interaction (competition) between the donor- and acceptor-stained mAbs because the same mAb is used for targeting the donor and the acceptor. One implication of the steric interaction is that the quenching value calculated as the relative decrease of donor intensity contains a contribution from the competition in addition to that of FRET; the other implication is that, in this case, the easy way of calculation by using $d_0 - d'$ instead of $d - d'$ in the quadratic equation for α (Eq. 9) gives only an approximation, being that the real d value is now unknown and smaller than d_0 for the donor-only sample. A way forward is offered by the knowledge of the functional form of intensity dependence of the donor moment on the donor intensity. It is formulated either by a plot of relative moment change versus relative intensity change ($Q' - Q$ plots) obtained on donor-labeled samples of different mean intensities, or in a self-contained manner, obtained on the double-labeled FRET sample itself by successive gating on an intensity parameter different

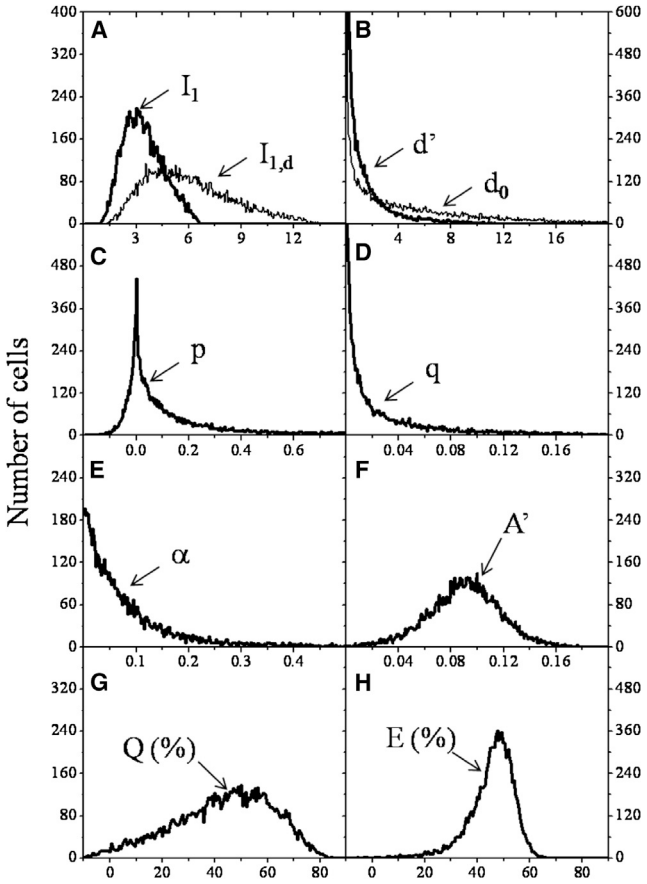

FIGURE 2 Representative histograms of covariance-based FRET determination. For the application of the quadratic equation (Eq. 9) for α, first the second moments (or variances) d' and d_0 are computed as mean values of the corresponding squared deviation (or fluctuation square) distributions (Panel *B*). In Panel *B*, d' and d_0 are distributions of the squared deviations from the respective means (or fluctuation squares) computed from the distribution of the donor intensity of the double-labeled FRET sample (I_1) and the donor-only one ($I_{1,d}$) of Panel *A*, respectively. Next, the p and q input constants for Eq. 9 are computed as averages of their respective distributions shown in Panels *C*, *D*. In Panel *C*, the distribution of p is that of the product of the deviations for I_1 (Panel *A*) and A' (Panel *F*) from their respective means. In Panel *D*, the distribution of q is that of the squared deviation of the $I_1 \cdot A'$ product from its mean value. In Panel *E* shown is the distribution of α as computed by a cell-by-cell solution of Eq. 9 with the input distributions d', p, q and with the average of the d_0 distribution as an input constant. As a summary, the distributions of d', p, q, A', and α (Panels *B-F*) are determined on the double-labeled FRET sample, distributions of I_1,d and d_0 (Panels *A*, *B*) on the donor-only sample. Finally, histogram of donor quenching efficiency Q (Panel *G*) is computed from the input histogram of I_1 and the average of $I_{1,d}$ as input constant according to $Q=1-I_1/I_{1,d}$. Histogram of FRET efficiency E (Panel *H*), taking into account both donor quenching and sensitized acceptor emission, is computed from the distribution of A' (Panel *F*) and the mean of the α distribution (Panel *E*) as input constant according to $E=A'/(\alpha+A')$. During analysis, all intensities were divided by 1000, meaning that all moments are divided by 10^6. The distributions (reminiscent to Weibull-type) are determined for the Alexa-Fluor 488-conjugated L368, Alexa-Fluor 546-conjugated W6/32 transfer pair labeling the β_2m and heavy-chain subunits of MHCI on the surface of FT T-lymphoblast cells. The details of the computations with the mean values of the shown distributions can be found in the Supporting Material.

from the I_1 intensity, e.g., the I_2, I_3 or the light scatter (FSC, SSC) intensities (so-called conditional-variance versus conditional-mean plots are discussed in the Supporting Material). The advantage of the knowledge of the functional dependence of the donor moment on the mean intensity is that the unperturbed donor moment on the double-labeled FRET sample can be expressed with the FRET efficiency E, or equivalently A' and α via Eq. S12 in the Supporting Material (Eq. 19). However, the price of estimation of the unknown d with a known functional form containing E is that the quadratic Eq. 9 turns into a cubic one (Eq. 20): hence the designation α_{cubic} for the α-factor obtained this way.

By examining FRET efficiencies obtained in the L368→W6/32 direction for the Alexa-Fluor 546-647 dye-pair (Table 1 *A*), it can be seen that whereas the quenching efficiency Q and the FRET efficiency E_0 calculated by using the conventional (or spectral) α_0 show a considerable difference, in the one calculated with the covariance-based α, E is practically the same as the quenching efficiency. It is also clear that this large difference in E values is attributed to the large difference in α-factors, α_0 being much larger than α. Importantly, because of the lack of competition, this observation implies also that the true value of the α-factor is obtained not with the conventional but with the believed-new method.

In contrast, in the reversed direction W6/32→L368 (Table 1 *B*), also a case of noncompeting mAbs, both FRET efficiencies E_0 and E are practically coinciding with the quenching efficiency Q. In parallel with the similar E values, the α-factors obtained with the two methods are also very close to each other. The contradicting observations observed in these FRET directions can only be resolved if we assume that the cause of the large difference in α-factors observed in the L368→W632 direction is due to the large labeling ratio of the donor-bearing L368 mAb ($L_d = 4.7$), which largely deviates from unity, as compared to the donor-bearing W6/32 mAb ($L_d = 1.5$) of the reversed FRET direction, and as compared to the acceptor-bearing W6/32 and L368 mAbs in both directions, which are almost the same and stay rather small (1.7 vs. 2.1).

The evaluation of data of the L368-L368 and W6/32-W6/32 pairs (Table 1 *C*) is more complicated: here the FRET efficiencies E_0 and E cannot be compared to the quenching efficiency Q, due to the competition. Here, again, whereas a large difference is seen between the conventional or spectral α-factors, implying a corresponding difference between the E_0 and E values, seemingly the covariance-based α-factor does not deviate much, implying also similarly large E values. The indicated E-values were calculated here not from α, but from α_{cubic} (obtained as a root of the cubic Eq. 20), which are a little larger than α, implying also correspondingly smaller E values.

Comparative measurements of FRET between epitopes of MHCI at different labeling ratios of mAbs on the surface of FT T-lymphoblast cells: II. Alexa-Fluor 488-546 dye pair

Please see the Supporting Material.

Comparative measurements of FRET between epitopes of MHCI at different labeling ratios of mAbs on the surface of LS174T cells

In addition to the FT cell line discussed above, analog experiments have been carried out on LS174T cells as a control, to demonstrate the stability of α determination with the correlation method. The influences of receptor expression levels and cluster densities as modified by IFNγ treatments have been considered (see Table S1 and additional details in the Supporting Material).

Correlating FRET indices Q, Q', E_0, and E

Because, in the case of intramolecular FRET measured between donor-labeled β_2m or light-chain and acceptor labeled heavy-chain subunits of MHCI, essentially there is no competition between the mAbs, simple donor quenching can be regarded as a FRET index, a parameter monotonously changing with the real FRET efficiency. It is calculated as the decrease of donor intensity (I_1) in the presence of acceptor, referenced to the mean intensity of the donor-only sample ($I_{1,d}$): $Q = 1 - I_1/I_{1,d}$ (quenching of intensity mean). Because the intensity moment of the donor is also expected to change monotonously with FRET, although with a different functional form, a FRET index can also be defined with the intensity moment d' for the double-labeled sample, and d_0 for the donor-only sample: $Q' = 1 - d'/d_0$ (quenching of intensity variance). Another two FRET indices are the conventional FRET efficiency E_0 calculated with the conventional α_0 and the intensity correlation-based FRET efficiency E calculated with the new α-value. Fig. 3 shows the plots for these FRET indices pooled for 34 different measurements as functions of each other to reveal trends in their behavior, involving the Alexa-Fluor 488-546, Alexa-Fluor 546-647, Alexa-Fluor 546-Cy5 dye-pairs, as donor-acceptor pairs attached to the light and heavy chains of the MHCI receptor on the surface of FT and LS174T cells.

As to the quenching efficiencies Q' and Q, Fig. 3 *A* reports on a rather good correlation between them (79.3%, the dependence is not strictly linear), implying that the intensity moments alone may also be used for quantifying FRET after calibration. This is expected, because by starting out from the definition of Q' and Q, it can be shown that

$$Q' = 1 - \mu \cdot (1 - Q)^2, \tag{25}$$

with

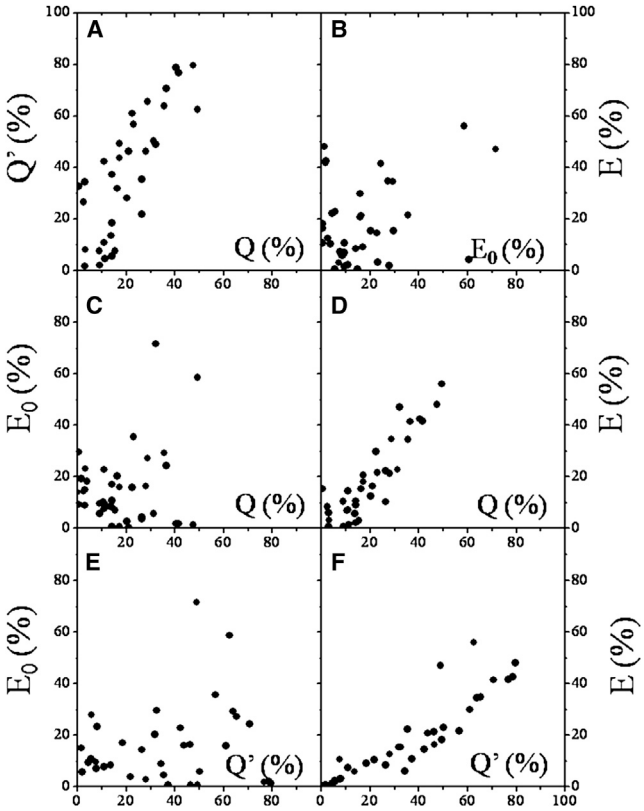

FIGURE 3 Scatter-plots of pooled data expressing the general trends in the degree of correlations between the different FRET indices. Values of different FRET indices (indicated with *dots*, each representing a different sample) have been put on a common scale for the L368-W6/32 and W6/32-L368 (practically noncompeting) antibody pairs stained with either the Alexa-Fluor 488/Alexa-Fluor 546 or the Alexa-Fluor 546/Alexa-Fluor 647 (or Cy5) dye-pair, for the LS174T and FT cell lines. The different FRET indices are as follows: Q', the relative change in the variance of donor intensity when the double-labeled sample is compared to the single donor-labeled one; Q, the relative change in the mean of donor intensity when the double-labeled sample is compared to the single donor-labeled one; E_0, FRET efficiency calculated by scaling A' with the conventional α-factor (or spectral α, α_0); and E, FRET efficiency calculated by scaling A' with the covariance-based α-factor. (*A*) Good correlation is between Q and Q' ($r(Q, Q') = 79.3\%$). (*D* and *F*) The correlations of E are good with both Q and Q' ($r(E, Q) = 88.8\%$, $r(E, Q') = 89.4\%$). (*B*, *D*, and *E*) However, the correlations of E_0 with E, Q, and Q' are bad ($r(E_0, E) = 44.9\%$, $r(E_0, Q) = 20.5\%$, and $r(E_0, Q') = 20.2\%$). Seemingly, in panel *B*, the correlations in these cases are ruined by points whose trend line is aligned approximately parallel with the horizontal and vertical axes, implying over- and underestimation of the real FRET efficiencies, due to the large acceptor and donor labeling ratios, respectively. For panels *C* and *E*, the opposite is true. This is supported by Fig. S6 in the Supporting Material directly showing the dependence of the FRET indices on the labeling ratios. Despite the good correlations of E with Q and Q', the individual dispersion of these quantities, and also that of E_0, is substantial, due to the different types of dye-pairs and the different acceptor levels dictated by the different labeling ratios of the acceptor-targeting mAbs (L_a) as well as the different surface expression levels of MHCI (homo-association of MHCI has a contribution to the intramolecular FRET).

$$\mu \equiv \frac{\overline{I_1^2}/\overline{I_1}^2 - 1}{\overline{I_{1,d}^2}/\overline{I_{1,d}}^2 - 1}, \tag{26}$$

where I_1 designates the donor intensity with acceptor, and $I_{1,d}$ without acceptor (essentially the ratio of squared coefficients of variation for I_1 and $I_{1,d}$, i.e., $CV_{I_1}^2$, and $CV_{I_{1,d}}^2$). After expanding the squared term, and neglecting the term containing Q^2 (this is allowed if $Q^2 \ll 1$), Eq. 25 reduces to

$$Q' \cong 1 - \mu + 2 \cdot \mu \cdot Q. \tag{27}$$

The same reasoning is also behind Eq. 18, when it was assumed that Q' can be written as a linear function of Q (keeping the term second-order in Q would lead to a fourth-power term in Eq. 20 for α if $\mu \neq 1$). The slope and intercept values of the linear trend-line fitting data points of Fig. 3 *A* are 1.568 ± 0.353 and 0.025 ± 0.078 ($R^2 = 0.661$), indicating that the assumption of the linearity is fulfilled with a good accuracy.

In contrast, essentially no correlation of E_0 with these quenching efficiencies Q and Q' is reported by Fig. 3, *C* and *D* (20.5%, 20.2%), due to the smearing effect of those mAbs having large labeling ratios. For the dependence of E, E_0, Q, and Q' on the labeling ratios L_d, L_a, and the L_d/L_a ratio, please consult Fig. S6 in the Supporting Material. However, for E, determined in a labeling ratio-free manner, good correlations are indicated with both Q (88.8%) and Q' (89.4%) in Fig. 3, *D* and *F*. That the correlation of E is better with Q' than with Q is supposedly because computation of each involves the donor-intensity moments. Finally, a poor correlation is seen between E and E_0 (44.9%) due to inflation by those mAbs having large labeling ratios. These plots demonstrate that the intensity correlation-based α is superior to the conventional α_0 for mAbs of large labeling ratio (see also Fig. S6).

Correlation plots of pooled data for FRET indices describing the L368-L368, and W6/32-W6/32 homo-associations (not shown) revealed similar trends between the correlations—namely that there is large correlation between Q and Q' (84.5%) and correlations of E are larger than those of E_0: $r(E, Q) = 78.4\%$, $r(E, Q') = 72.9\%$, $r(E_0, E) = 26.8\%$, $r(E_0, Q) = 11.3\%$, and $r(E_0, Q') = 12.2\%$.

Fluorescence lifetime depends on the labeling ratios of mAbs

Data obtained by FLIM directly demonstrate that light emission by ligand-bound dyes is affected by the dye-per-protein labeling ratio (see Fig. S5 and details in the Supporting Material). Due to the interactions between dyes, the assumption of linearity between dye concentration and fluorescence intensity may not be fulfilled, and as a consequence, the form of Eq. 2 for α determination may be violated.

DISCUSSION

Intensity correlations offer new degrees of freedom for calibrating FRET measurements

Flow cytometry is a technology inherently applicable to developing methods based on the concept of intensity fluctuations, being that the outputs of this technology are the probability distribution functions describing the different cell parameters at the level of populations. Despite this advantage offered by flow cytometry, intensity correlations that were manifested in the width of the intensity distribution curves, a scale parameter (31,32) of the distributions, have not been exploited explicitly to extend the capabilities of measurements, the majority of which concentrated on the determination of some location parameters, the mean, median, or mode.

The impetus to this work was given by a need to extend the capabilities of the FCET method, originally worked out by Trón and co-workers (7,8) to determine FRET efficiency by concentrating only on a single sample, namely on the double-labeled FRET sample. To put it another way, we were trying to reduce the number of spectroscopic-optical constants—the input parameters of FRET determination—from non-FRET samples as much as possible, to determine FRET in a self-consistent manner. However, to fulfill this requirement, finding extra parameters as yet not involved in FRET determination, like some measure of intensity correlations, is necessary. An advantage of determining a spectroscopic constant based on the intensity correlations (as a scale parameter) instead of intensity means (as a location parameter) can also be expected, namely that whereas the location parameters are off-set dependent (e.g., the subtracted background), the scale parameters are not, with the consequence of increasing accuracy of the determination of the given spectroscopic constant and ultimately the deduced FRET efficiency.

According to the scheme of the dual-laser (or dual-wavelength) FCET method (detailed in the Supporting Material), FRET efficiency is determined from intensities of the double-labeled FRET sample in the knowledge of the S_1, S_2, and S_3 spillage factors and the scaling factor α (Eq. 2, and see Eqs. S4–S6 in the Supporting Material), all of them determined in advance from single donor- and single acceptor-labeled samples measured in the same spectroscopic (the same dyes) and optical conditions (equipment state). Among these constants, α is the candidate, the determination of which is amenable to being put on the basis of intensity correlations. This is because α is the balancing factor between the different sensitivities of donor and acceptor signal channels, so it also plays an inherent role in shaping the width of the intensity distributions. In addition to this, the role of α is the proper scaling of the A' parameter directly determined from the primarily measured I_1, I_2, and I_3 intensities (see Eq. S10 in the Supporting Material), which after scaling, directly determines the FRET efficiency (see Eq. S12 in the Supporting Material). The α-value also directly connects the width of the deduced FRET efficiency distribution with that of A' via

$$\Delta E = \alpha \cdot \left(E/A'\right)^2 \cdot \Delta A' \tag{28}$$

(obtainable from Eq. S12 in the Supporting Material), where ΔE and $\Delta A'$ designate the standard deviation (proportional to the distribution width) of E and A', respectively.

The FCET method, originally elaborated upon in the field of flow cytometry, can be adapted in fluorescence microscopy (33), as is also the case with our intensity-correlation extension, based on the image pixel-cell correspondence. Especially in microscopy, combining the FCET approach with the acceptor photobleaching version of FRET determination (34) may offer promise. Because both the donor moments, with and without FRET (d' and d), necessary for determination of α, can be measured in the same pixels, the distribution of $D = d - d'$ can also be determined in a pixel-by-pixel manner. This circumstance eliminates the need for estimating d with d_0 the donor-only moment, or any assumption on a dependence of d on E (Eq. 19).

A similar approach could also be used in multiparameter flow cytometry, e.g., when the acceptor of the FRET sample would be bleached out with an intensive beam of light. Although in this case d' and d would be measured sequentially (the cells first passing a probe laser beam, then a bleaching beam), the signals would be correlated. Here the $D = d - d'$ difference could be determined on a cell-by-cell basis, increasing accuracy compared to the case when the d donor moment without FRET is approximated with the d_0 moment of the single-donor labeled sample.

The approach of applying intensity correlations for extending capabilities of FRET determination was also followed by Esposito et al. (35) in the field of FLIM. They worked out a method that is conceptually similar to ours, but totally different in details of mathematical formalism and the aimed parameter: They used the moment analysis for extending the resolution of the FRET data by determining the fraction of donors associated with acceptors (i.e., FRET fraction).

Overview of the correlation method

Please see the Supporting Material.

Comparative measurements of FRET at different labeling ratios of mAbs reveal differences in the conventional and covariance-based FRET determinations

Possible causes of the difference between the conventional and the correlation-based methods for α determination

(see Fig. S6)—such as nonlinear concentration dependence of light emission and shielding of binding sites—are discussed in the Supporting Material.

Advantages of the intensity correlation-based FRET method

By comparing the defining Eqs. 2 and 9 for α, the following basic differences can be recognized:

1. The correlation-based α factor (Eq. 9) does not depend on the ligand labeling ratios, implying that the error caused by the lack of knowledge of the effective labeling ratio drops out.
2. Because α is computed from deviations from the means (intensity fluctuations), disturbing effects of bad zero-offsets (bad background subtractions) cancel, but not in the conventional formula (Eq. 2).
3. For using the conventional formula Eq. 2, knowledge of the numbers of the labeled receptors (or at least their ratio) is necessary on the FRET sample. However, there are cases when this is unknown: e.g., when genetically engineered VFPs are expressed on the cell surface. However, the believed-new method also offers a remedy in these cases, because the need for the precise knowledge of the quantity d on the FRET sample can be replaced by a weaker condition of the need for knowing only the functional dependence of d on the mean intensity (i.e., intensity variance versus intensity mean titration plots), which can be recorded if several donor-only samples of different, but not necessarily known, receptor expression levels are available. In the linear approximation of this dependence, Eq. 9 turns into a cubic one (Eq. 20). An approximation of the required donor-intensity-variance versus intensity-mean-titration plots can also be taken up by using only the double-labeled FRET sample. The total population of the cell sample is divided into monotonously increasing subpopulations by successive gating on a second parameter (e.g., I_2, I_3, FSC, SSC), and the variance of I_1 is plotted against the mean of I_1 for these subpopulations, resulting in plots (conditional-variance versus conditional-mean plots), which can be fitted by an exponential trend line with high accuracy ($R^2 > 90\%$). Then the moment difference D can be expressed with α via this trend line and put into Eq. 9, leading to the transcendental Eq. S18 (in the Supporting Material) for α.
4. Even in the lack of any knowledge on a functional form of the variation of intensity moment with intensity mean, lower and upper bounds for α can be obtained by replacing D in Eq. 9 by its maximum value $D_{max} = d_0$ ($D = d - d' < d_0 - d' = d_0$ when $E = 100\%$, and $d' = 0$) leading to minimal α and its minimum value $D_{min} = 0$ ($D = d - d' = 0$ when $E = 0\%$, and $d' = d$) leading to maximal α, respectively.

CONCLUSION

A believed-novel approach of FRET determination based on fluorescence intensity correlations has been elaborated for the first time, to our knowledge, by using flow cytometry and immunolabeling of cells. The believed-new method was demonstrated to be superior to the old one in that:

1. It does not involve the knowledge of the effective labeling ratio of the used dye-conjugates for computation of the α-factor as an input parameter; rather, it allows the determination of it.
2. It allows the estimation of FRET efficiency by using only the double-labeled FRET sample for estimation of α.
3. Being a way of determination of α that is free from receptor density, it also allows the usage of the FCET method when receptor density is not known, e.g., in the cases of engineered VFPs. Although elaborated in flow cytometry, it can straightforwardly be adapted in fluorescence microscopy.

SUPPORTING MATERIAL

Two tables, ten figures, references (36–46) and supplemental information are available at http://www.biophysj.org/biophysj/supplemental/S0006-3495(13)01089-8.

Thanks are due to Ms. Rita Szabó for her skillful assistance in cell culturing and sample preparations, to Dr. J. Szöllősi for his helpful comments on the manuscript, and to a Reviewer for drawing our attention to the work of Ranjit et al. (13) and Lewis et al. (14).

Financial support for this work was provided by the TÁMOP-4.2.2.A-11/1/KONV-2012-0045 project cofinanced by the European Union and the European Social Fund. The authors are indebted to Dr. T. M. Jovin for making possible FLIM measurements of the dye-conjugated mAbs in the framework of a short-term EMBO fellowship (No. ASTF No 201-06 to L.B.) to the Max Planck Institute for Biophysical Chemistry, Department of Molecular Biology, Göttingen.

REFERENCES

1. Lakowicz, J. R. 2006. Ch. 13: Energy transfer. *In* Principles of Fluorescence Spectroscopy, 3rd Ed. Springer, New York, pp. 443–472.
2. Jares-Erijman, E. A., and T. M. Jovin. 2003. FRET imaging. *Nat. Biotechnol.* 21:1387–1395.
3. Clegg, R. M. 2009. Ch. 1: Förster resonance energy transfer-FRET: what is it, why do it, and how it's done. *In* FRET and FLIM Techniques. Laboratory Techniques in Biochemistry and Molecular Biology, *Vol. 33*. T. W. J. Gadella, S. Pillai, and P. C. van der Vliet, editors. Elsevier, Dordrecht, The Netherlands, pp. 1–48.
4. Bacsó, Z., L. Bene, …, S. Damjanovich. 1996. A photobleaching energy transfer analysis of CD8/MHC-I and LFA-1/ICAM-1 interactions in CTL-target cell conjugates. *Immunol. Lett.* 54:151–156.
5. Bene, L., M. J. Fulwyler, and S. Damjanovich. 2000. Detection of receptor clustering by flow cytometric fluorescence anisotropy measurements. *Cytometry.* 40:292–306.
6. Bene, L., J. Szöllősi, …, S. Damjanovich. 2005. Detection of receptor trimers on the cell surface by flow cytometric fluorescence energy homotransfer measurements. *Biochim. Biophys. Acta.* 1744:176–198.
7. Trón, L., J. Szöllősi, …, T. M. Jovin. 1984. Flow cytometric measurement of fluorescence resonance energy transfer on cell surfaces.

Quantitative evaluation of the transfer efficiency on a cell-by-cell basis. *Biophys. J.* 45:939–946.

8. Trón, L. 1994. Experimental methods to measure fluorescence resonance energy transfer. *In* Mobility and Proximity in Biological Membranes. S. Damjanovich, J. Szöllősi, L. Trón, and M. Edidin, editors. CRC Press, Boca Raton, FL, pp. 1–47.
9. Szöllősi, J., S. Damjanovich, and L. Mátyus. 1998. Application of fluorescence resonance energy transfer in the clinical laboratory: routine and research. *Cytometry.* 34:159–179.
10. Nagy, P., L. Bene, …, J. Szöllósi. 2005. Novel calibration method for flow cytometric fluorescence resonance energy transfer measurements between visible fluorescent proteins. *Cytometry A.* 67:86–96.
11. Vámosi, G., N. Baudendistel, …, K. Tóth. 2008. Conformation of the c-Fos/c-Jun complex in vivo: a combined FRET and MD-modeling study. *Biophys. J.* 94:2859–2868.
12. Szalóki, N., Q. M. Doan-Xuan, …, Z. Bacsó. 2013. High throughput FRET analysis of protein-protein interactions by slide-based imaging laser scanning cytometry. *Cytometry A.* 83:818–829.
13. Ranjit, S., K. Gurunathan, and M. Levitus. 2009. Photophysics of backbone fluorescent DNA modifications: reducing uncertainties in FRET. *J. Phys. Chem. B.* 113:7861–7866.
14. Lewis, F. D., L. Zhang, and X. Zuo. 2005. Orientation control of fluorescence resonance energy transfer using DNA as a helical scaffold. *J. Am. Chem. Soc.* 127:10002–10003.
15. Rényi, A. 1959. On measures of dependence. *Acta. Math. Acad. Sci. Hungary.* 10:441–451.
16. Feller, W. 1968. Ch. IX: Random variables: expectations. *In* An Introduction to Probability Theory and its Applications, *Vol. I*, 3rd Ed. John Wiley & Sons, New York, pp. 212–237.
17. Feller, W. 1970. Ch. V: Probability distributions in R^{r}. *In* An Introduction to Probability Theory and its Applications, *Vol. II*, 2nd Ed. John Wiley & Sons, New York, pp. 127–165.
18. Horváth, G., M. Petrás, …, J. Szöllősi. 2005. Selecting the right fluorophores and flow cytometer for fluorescence resonance energy transfer measurements. *Cytometry A.* 65:148–157.
19. Szentesi, G., G. Horváth, …, L. Mátyus. 2004. Computer program for determining fluorescence resonance energy transfer efficiency from flow cytometric data on a cell-by-cell basis. *Comput. Methods Programs Biomed.* 75:201–211.
20. Kerker, M., M. A. van Dilla, …, R. G. Langlois. 1982. Is the central dogma of flow cytometry true: that fluorescence intensity is proportional to cellular dye content? *Cytometry.* 3:71–78.
21. Hirschfeld, T. 1976. Quantum efficiency independence of the time integrated emission from a fluorescent molecule. *Appl. Opt.* 15:3135–3139.
22. Deka, C., B. E. Lehnert, …, J. A. Steinkamp. 1996. Analysis of fluorescence lifetime and quenching of FITC-conjugated antibodies on cells by phase-sensitive flow cytometry. *Cytometry.* 25:271–279.
23. MacDonald, R. I. 1990. Characteristics of self-quenching of the fluorescence of lipid-conjugated rhodamine in membranes. *J. Biol. Chem.* 265:13533–13539.
24. Lakowicz, J. R. 2006. Ch. 3: Fluorophores. *In* Principles of Fluorescence Spectroscopy, 3rd Ed. Springer, New York, pp. 63–94.
25. Kenny, D. A. 1979. Ch. 2: Covariance algebra. *In* Correlation and Causality, 1st Ed. John Wiley & Sons, New York, pp. 16–26.
26. Kullback, S. 1997. Ch. 2: Properties of information. *In* Information Theory and Statistics Dover, Mineola, NY, pp. 12–31.
27. Wallrabe, H., M. Elangovan, …, M. Barroso. 2003. Confocal FRET microscopy to measure clustering of ligand-receptor complexes in endocytic membranes. *Biophys. J.* 85:559–571.
28. Hanley, Q. S., V. Subramaniam, …, T. M. Jovin. 2001. Fluorescence lifetime imaging: multi-point calibration, minimum resolvable differences, and artifact suppression. *Cytometry.* 43:248–260.
29. Gáspár, Jr., R., P. Bagossi, …, S. Damjanovich. 2001. Clustering of class I HLA oligomers with CD8 and TCR: three-dimensional models based on fluorescence resonance energy transfer and crystallographic data. *J. Immunol.* 166:5078–5086.
30. Damjanovich, S., L. Bene, …, J. Szöllősi. 1999. Two-dimensional receptor patterns in the plasma membrane of cells. A critical evaluation of their identification, origin and information content. *Biophys. Chem.* 82:99–108.
31. Lindley, D. V. 1969. Ch. 2.4: Features of distributions. *In* Introduction to Probability and Statistics from a Bayesian Viewpoint. Part 1: Probability Cambridge University Press, Cambridge, UK, pp. 74–82.
32. Huber, P. J., and E. M. Ronchetti. 2009. Ch. 8: Robust covariance and correlation matrices. *In* Robust Statistics, 2nd Ed. John Wiley, New York, pp. 199–237.
33. Nagy, P., G. Vámosi, …, J. Szöllősi. 1998. Intensity-based energy transfer measurements in digital imaging microscopy. *Eur. Biophys. J.* 27:377–389.
34. van Munster, E. B., G. J. Kremers, …, T. W. Gadella, Jr. 2005. Fluorescence resonance energy transfer (FRET) measurement by gradual acceptor photobleaching. *J. Microsc.* 218:253–262.
35. Esposito, A., H. C. Gerritsen, and F. S. Wouters. 2005. Fluorescence lifetime heterogeneity resolution in the frequency domain by lifetime moments analysis. *Biophys. J.* 89:4286–4299.
36. Hori, T., T. Uchiyama, …, H. Uchino. 1987. Establishment of an interleukin 2-dependent human T cell line from a patient with T cell chronic lymphocytic leukemia who is not infected with human T cell leukemia/lymphoma virus. *Blood.* 70:1069–1072.
37. Szöllősi, J., V. Horejsí, …, S. Damjanovich. 1996. Supramolecular complexes of MHC class I, MHC class II, CD20, and tetraspan molecules (CD53, CD81, and CD82) at the surface of a B cell line JY. *J. Immunol.* 157:2939–2946.
38. Tanabe, M., M. Sekimata, …, M. Takiguchi. 1992. Structural and functional analysis of monomorphic determinants recognized by monoclonal antibodies reacting with the HLA class I α3 domain. *J. Immunol.* 148:3202–3209.
39. Szöllősi, J., S. Damjanovich, …, F. M. Brodsky. 1989. Physical association between MHC class I and class II molecules detected on the cell surface by flow cytometric energy transfer. *J. Immunol.* 143:208–213.
40. Edidin, M., and T. Wei. 1982. Lateral diffusion of H-2 antigens on mouse fibroblasts. *J. Cell Biol.* 95:458–462.
41. Bene, L., M. Balázs, …, S. Damjanovich. 1994. Lateral organization of the ICAM-1 molecule at the surface of human lymphoblasts: a possible model for its co-distribution with the IL-2 receptor, class I and class II HLA molecules. *Eur. J. Immunol.* 24:2115–2123.
42. Bacsó, Z., L. Bene, …, S. Damjanovich. 2002. INF-γ rearranges membrane topography of MHC-I and ICAM-1 in colon carcinoma cells. *Biochem. Biophys. Res. Commun.* 290:635–640.
43. Bene, L., Z. Kanyári, …, L. Damjanovich. 2007. Colorectal carcinoma rearranges cell surface protein topology and density in $CD4^{+}$ T cells. *Biochem. Biophys. Res. Commun.* 361:202–207.
44. Bojarski, C., and K. Sienicki. 1989. Ch. 1: Energy transfer and migration in fluorescent solutions. *In* Photochemistry and Photophysics, *Vol. I.* CRC Press, Boca Raton, FL, pp. 1–56.
45. Murphy, R. M., H. Slayter, …, M. L. Yarmush. 1988. Size and structure of antigen-antibody complexes. Electron microscopy and light scattering studies. *Biophys. J.* 54:45–56.
46. Rényi, A. 1981. Ch. IV: Arbitrary random variables. *In* Probability Theory, 4th Ed. Tankönyvkiadó, Budapest, Hungary, pp. 161–238.

Supplement to „ Intensity correlation-based calibration of FRET" (by L. Bene et al.)

Glossary of symbols

α_0: "spectroscopic" α-factor determined with the conventional way, Eq. 2;
α: α-factor determined with the correlation-based quadratic equation, Eq. 9;
α_{cubic}: α-factor determined with the correlation-based cubic equation, Eq. 20;
ε_d, ε_a: molar decadic extinction coefficients, for donor (d) and acceptor (a);
B_d, B_a: number of labeled binding sites, for donor (d) and acceptor (a);
L_d, L_a: dye/protein labeling ratios, for donor (d) and acceptor (a);
I_1, I_2, I_3: intensities in the donor channel, in the channel of sensitized emission, and in the acceptor channel, respectively;
I_d: unquenched donor intensity of the FRET sample;
M_d, M_a: mean values of intensities I_1 and I_2 of the single-labeled samples, for donor (d) and acceptor (a);
E: FRET efficiency as determined by the combined donor quenching and sensitized emission in the FCET method;
S_1, S_2, S_3: spectral spillage factors determined from single-labeled samples, Eqs. 4s-6s;
A': primarily determined FRET-related quantity of the FCET method from which FRET efficiency E is calculated as $E=A'/(\alpha+A')$, Eq. 10s;
d_0: second central moment, variance of the donor intensity of the single donor-labeled sample $I_{1,\text{ donor only}}$, $d_0=(I_1, I_1)_{\text{donor only}}$;
d': second central moment, variance of the quenched donor intensity of the FRET sample I_1, $d=(I_1, I_1)$;
d: second central moment, variance of the unquenched donor intensity of the FRET sample I_d, $d=(I_d, I_d)$;
D: difference of central moments for unquenched and quenched donor intensities d and d', D=d-d';
(ξ, ψ): covariance of the ξ and ψ random variables;
p: covariance of I_1 and I_1A', (I_1, I_1A');
q: variance of I_1A', (I_1A', I_1A');
Q: quenching efficiency calculated from donor intensity, Eq. 16;
Q': quenching efficiency calculated from second moments of donor intensity, Eq. 17;
m: slope of linear trend line fitting the Q' vs. Q plot, Eq. 18;
b: intercept of linear trend line fitting the Q' vs. Q plot, Eq. 18;
d_a': second central moment of acceptor without FRET calculated from I_a, Eq. 29s;
d_a'': second central moment of acceptor with FRET calculated from I_a and I_1A', Eq. 30s;
p_i, i=0, 1, 2, 3: coefficient of the i^{th} order term in the cubic equation for α_{cubic}, Eqs. 21-24;
CV_ξ: coefficient of variation for random variable ξ, $CV_\xi = \sqrt{(\xi,\xi)}/\overline{\xi}$, Eqs. 37s-39s, 53s-55s.

Organization of paper

As to the organization of the main text, in the *Theoretical results* part first a quadratic equation for α is deduced. Then its properties are discussed for sterically interacting and non-interacting (competing vs. non-competing) dye-targeting labels (mAbs). For competing labels estimation of the moment of the donor-only sample in the coefficient of the leading term quadratic in α is given based on: (i) Experimentally recorded modulation of variance (2^{nd} moment) of donor intensity vs. mean intensity („Q'-Q plots"). (ii) Observed modulation of variance of donor intensity vs. mean intensity for subpopulations of the double-labeled FRET sample defined by a successively increasing gate series defined on the intensity scale of sensitized emission („conditional variance" vs. „conditional mean" plots in the *Supplement*).

In the *Experimental results* part, α factors determined in the conventional and the new way are compared: (i) For different labeling ratios of the donor- and acceptor-stained mAbs against the β_2m and heavy chain (h.c.) subunits of the MHCI cell surface receptor. (ii) For two different donor-acceptor dye-pairs (Alexa-Fluor 488-Alexa-Fluor 546 vs. Alexa-Fluor 546-Alexa-Fluor 647, in *Supplement*) to change Förster's R_0 expressing the spectral overlap between the donor and acceptor dyes. (iii) For two different cell lines (FT and LS174T cells) and for treatments of LS174T cells with IFNγ (in *Supplement*) to change the donor intensity levels as well as FRET efficiency via modulation of the surface expression levels of MHCI.

In the *Supplement* we first briefly summarize the conventional FCET method, then a case study is presented as an illustration. An alternative deduction is made of the quadratic equation for α by a unified treatment of the modulations of the donor and acceptor signals during the FRET process. An information theoretical meaning has also been attached to the donor and acceptor moments. Fluorescence lifetime data demonstrating labeling ratio dependence of quantum efficiency and error analysis illustrating stability of α determined as roots of the respective quadratic and cubic equations are presented.

Cells

LS174T colon carcinoma cells (ATCC, Manassas, VA) were kept in continuous logarithmic growth in RPMI 1640 medium supplemented with 10% FCS and 50 μg/ml gentamycin by sub culturing them twice weekly at a concentration of $2.5x10^4$ cells/cm^2 with standard trypsinization. For cell activation experiments, cells after sub culturing were treated with 50 ng/ml interferon-γ (IFNγ) (R&D Systems, Minneapolis, MN) and were cultured for an additional 48 h. Kit-225 FT7.10 (FT) cells, a human T-lymphotrophic virus-nonexpressing, cytokine-dependent (IL-2 or IL-15) human adult T lymphoma cell line with a $CD4^+$ phenotype derived from Kit-225 cells [1] were cultured in RPMI medium 1640 supplemented with 10% FBS, penicillin, and streptomycin. We also added 500 pM human recombinant IL-2 to the medium every 48 h. The medium of FT7.10 cells contained 800 μg/ml G418 (GIBCO) to suppress the growth of wild type cells.

Specificity of monoclonal antibodies

The production and specificity of monoclonal antibodies applied in the experimental procedures have been described earlier [2]. Briefly, mAbs W6/32 ($IgG_{2a\kappa}$) and L368 ($IgG_{1\kappa}$) developed against the heavy chain (h.c.) component of the MHCI molecule binding to a monomorphic epitope on the α_2, α_3 domains [3] and the β_2-microglobulin component of MHCI light chain (l.c.), respectively [4], were kindly provided by Dr. Frances Brodsky (UCSF, CA). Fab fragments were prepared from IgGs by papain digestion and were separated from the Fc fragments on protein A-Sepharose column using the method described earlier [5].

Fluorescent staining of mAbs

Aliquots of mAbs and purified Fab fragments were labeled with Alexa-Fluor and indocarbocyanine dyes (Alexa-Fluor 488 as donor, Alexa-Fluor 546 as acceptor or donor, Alexa-Fluor 647 as acceptor, from Invitrogen; Cy5 as acceptor, from Amersham). Kits provided with the dyes were used for the labeling. The detailed staining procedure was described earlier [4-8]. Dye to protein labeling ratios, when asterisk (*) indicates Fab fragments, were: L_d(Alexa-488-L368)=1.1*, 4.9; L_d(Alexa-488-W6/32)=0.85*, 3.4; L_a(Alexa-546-L368)=4.15, 4.7; L_a(Alexa-546-W6/32)=1.5, 2.5; L_a(Alexa-647-L368)=2.1, 5.8; L_a(Alexa-647-W6/32)=1.01*, 1.56, 1.7; L_a(Cy5-L368)=4.2; L_a(Cy5-W6/32)=4.7. The labeling ratios were separately determined for each labeled aliquot in a spectrophotometer (Hitachi U-2900, NanoDrop ND-1000) [2-6]. The labeled proteins retained their affinity as proven by competition experiments with identical, unlabeled ligands.

Labeling of cells with fluorescent ligands

Freshly harvested cells were washed twice in ice cold PBS (pH 7.4). The cell pellet was suspended in 100 μl of PBS (10^6 cells/ml) and labeled by incubation with 10 μg of dye-conjugated ligands (whole mAbs, Fab fragments) for 40 min on ice in the dark [2-6]. The excess of whole mAbs or Fabs was at least 30-fold above the K_d during incubation. To get rid

of possible aggregations of dye-conjugated ligands, they were air-fuged (at 110,000 g, for 30 min) before cell labeling. Labeled cells were washed twice with ice cold PBS and then fixed with 1%-formaldehyde/PBS. Special care was taken to keep the cells at ice cold temperature before FRET measurements in order to avoid unwanted induced aggregations of cell surface receptors or receptor internalization. Data obtained with fixed cells did not differ significantly from those of unfixed, viable cells.

Theory of dual-wavelength flow cytometric resonance energy transfer (FCET)

In the scheme of the FCET method originally published by L. Trón *et al.* in 1984 [9, 10], the energy transfer problem poses the determination of three unknowns on the acceptor and donor labeled cell samples, the donor and acceptor concentrations (represented by signals I_d and I_a bellow) as well as the energy transfer efficiency (E) from three suitable signals (I_1, I_2, I_3) after taking into account the necessary spectral overspills (S_1, S_2, S_3) as „natural characteristics" of FRET-pairs having large enough spectral overlaps. For a summary of the FCET method with the forthcoming extensions, please see also Fig. 1 in the main text. The system of equations contains also a very important 4^{th} parameter, called α, comparing the detectibilities (or „visibilities") of the donor and acceptor signals, whose determination is the central problem in this communication. The I_1 signal (all signals are already background-subtracted), excited at the donors absorption maximum and detected at its emission maximum is the donor fluorescence reduced by possible FRET towards acceptor (quenching) and modified by possible steric interactions between the donor and acceptor targeting labels,

$$I_1 = I_d \cdot (1 - E), \tag{1s}$$

where I_d is the donor fluorescence unperturbed by FRET, but potentially containing the effects of possible steric interactions, and E is the FRET efficiency. Signal I_2, excited at the donor's absorption maximum and detected at the acceptors emission maximum can be decomposed into a first term representing the overspill of the donor emission with the acceptor channel, a second term expressing direct photonic excitation of acceptor at the donor's excitation wavelength, and a third term representing the transferred energy (sensitized emission):

$$I_2 = I_d \cdot (1 - E) \cdot S_1 + I_a \cdot S_2 + I_d \cdot E \cdot \alpha. \tag{2s}$$

The determination of the three unknown parameters requires also a 3^{rd} equation, analogous to Eq. 2s, which is the signal I_3 emitted in the acceptor channel, but excited at the absorption maximum of the acceptor:

$$I_3 = I_d \cdot (1 - E) \cdot S_3 + I_a + I_d \cdot E \cdot \alpha \cdot S_3 / S_1 . \tag{3s}$$

In Eqs. 2s and 3s, S_1 and S_3 spectral spillage factors determined as

$$S_1 = (I_2 / I_1)_{\text{only donor}}, \tag{4s}$$

$$S_3 = (I_3 / I_1)_{\text{only donor}} \tag{5s}$$

on samples labeled only with the donor (also obtainable from Eqs. 2s and 3s by plugging 0 for E, and I_a). Factor S_2, which compares the excitabilities of acceptor at the donor's and

acceptor's excitation wavelength (acceptor's bleed through in the donor's excitation channel), can be determined on the sample labeled only with the acceptor according to

$$S_2 = \left(I_2/I_3\right)_{\text{only aceptor}}, \tag{6s}$$

as it can be deduced also from Eq. 2s or 3s by plugging zero for E and I_d. With the aid of these parameters, determined by the spectroscopy of the donor and acceptor and the actual optical alignment of the flow cytometer (or microscope), and with the α-factor, detailed later, Eqs. 1s-3s can be solved for E, I_d, and I_a on the double-labeled sample on a cell-by-cell basis in flow cytometry (or in a pixel-by-pixel basis in microscopy) by first introducing a „helper parameter" called A', which plays a crucial role in the elaboration of the present method:

$$A' = E \cdot \alpha/\left(1-E\right). \tag{7s}$$

Then expressing I_d from Eq. 1s and inserting into Eqs. 2s, 3s a system of two equations results,

$$I_2 = I_1 \cdot S_1 + I_a \cdot S_2 + I_1 \cdot A', \tag{8s}$$

$$I_3 = I_1 \cdot S_3 + I_a + I_1 \cdot A' \cdot S_3/S_1, \tag{9s}$$

which are conveniently solvable for the unknowns A' and I_a:

$$A' = \frac{I_2 - S_2 \cdot I_3}{\left(1 - S_2 \cdot S_3/S_1\right) \cdot I_1} - S_1, \tag{10s}$$

$$\mathrm{I_a} = \frac{\mathrm{I_3} - \mathrm{I_2} \cdot \mathrm{S_3}/\mathrm{S_1}}{1 - \mathrm{S_2} \cdot \mathrm{S_3}/\mathrm{S_1}}. \tag{11s}$$

Remarkable feature of A' and I_a is that the formulae for their experimental determination (Eqs. 10s, 11s) do not contain α, in spite of the involvement of α in the definition of A' (Eq. 7s). With the aid of A', E is expressed from Eq. 7s as

$$E = A'/\left(\alpha + A'\right), \tag{12s}$$

and finally by plugging E into Eq. 1s, I_d is obtained as:

$$I_d = I_1/\left(1-E\right). \tag{13s}$$

As it can be seen from Eq. 12s, the α-factor plays a crucial role in the determination of energy transfer efficiency: by comparing Eq. 12s with the „Förster-equation" $E=R_0^6/(R_0^6+R^6)$, A'/α can be identified with $(R_0/R)^6$ – in the original publication of the FCET method A'/α is designated by „A" defined as A=E/(1-E).

A case study on the gating strategy and computation of FRET efficiency in the FCET scheme

The FRET efficiencies, conventional E_0 and correlation-based E, are computed from the background-corrected I_1 (excited at the absorption maximum and detected at the emission maximum of donor, "donor channel"), I_2 (excited at the absorption maximum of the donor and detected at the emission maximum of the acceptor, channel of sensitized emission of acceptor or

"FRET channel"), and I_3 (excited at the absorption maximum and detected at the emission maximum of acceptor, "acceptor channel") intensities of the samples labeled with both donor and acceptor. Computations were done on a cell-by-cell basis by using Eqs. 10s, 12s and for α either Eq. 2 in the main text for the conventional E_0, or Eqs. 9, 20 for the correlation-based E, for the latter also with the assumption that the unperturbed donor moment of the doubly-labeled FRET sample equals that of the donor-only sample i.e. $d=d_0$ (see also Eq. 15 in the main text). Corrections for the spectral overlaps in absorption and emission of the donor and acceptor ("spectral demixing") are made by using the S_1, S_2, and S_3 "spillage factors", which are determined on samples labeled with only the donor (S_1, S_3) or the acceptor (S_2) according to Eqs. 4s-6s. The difference in sensitivities of the donor and FRET channels in detecting a single photon is taken into account with the "scaling factor" α (introduced by Eqs. 2s, 3s) which is determined on the samples labeled with only the donor or the acceptor according to Eq. 2 (conventional way leading to "spectral α" or α_0) and on the double-labeled FRET sample according to Eq. 9 ("correlation-based" leading to α) .

The steps of computation of flow cytometric FRET efficiencies and the necessary gating are illustrated with a case study on the Alexa-Fluor 488-L368 (anti-β_2m)-Alexa-Fluor 546-W6/32 (anti-MHCI h.c.) FRET pair on FT human T-lymphoblast cells. For the computation of a FRET efficiency the following 4 samples are needed with the cell-labeling donor and acceptor mAbs in parentheses:

1. *background* sample (unlabeled with donor or acceptor),
2. *donor* sample (labeled only with Alexa-Fluor 488-L368),
3. *acceptor* sample (labeled only with Alexa-Fluor 546-W6/32), and
4. *FRET* sample (labeled with both Alexa-Fluor-488 L368 and Alexa-Fluor 546-W6/32).

The details of calculations with the used dot-plots and gates are described in Figs. 1s-4s for the common steps of the two approaches. Histograms characteristic to the "correlation-based" approach are shown in Fig. 2 of the main text. All analyses were made with a home-made software ReFlex [11] freely available at http://www.biophys.dote.hu/research.htm or http://www.freewebs.com/cytoflex.htm.

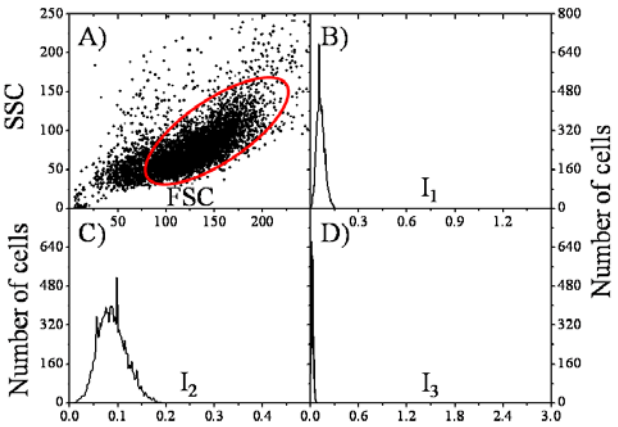

Fig. 1s *Background sample.* The major subpopulation comprising c.a. 80% of the total population of the heterogeneously growing FT cells was separated from the remaining cells and debris based on a gate (red ellipsis) put in the forward light scatter (FSC)-side scatter (SSC) dot-plot. The mean background values as computed from histograms I_1, I_2 and I_3 after activating the above gate – or if necessary from dot-plots I_1-I_2 and I_1-I_3 after putting another two "fine gates" (not shown) in these dot-plots to get reed of outliers – are: B_1=0.643, B_2=0.887, and B_3=0.252. All measured intensities are divided by 1000. These values are subtracted from all fluorescence intensities of the subsequent samples.

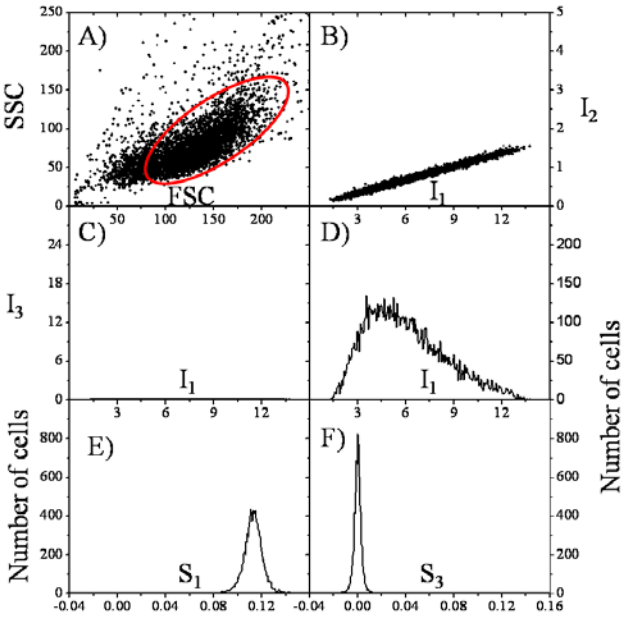

Fig. 2s *Donor sample.* The major subpopulation comprising c.a. 80% of the total population of the heterogeneously growing FT cells was separated from the remaining cells and debris based on a gate (red ellipsis) put in the forward light scatter (FSC)-side scatter (SSC) dot-plot. The I_1-I_2 and I_1-I_3 dot-plots are computed by activating the "initial gate", from which the $S_1=I_2/I_1$ and $S_3=I_3/I_1$ histograms are computed – if necessary, after by activating two additional "fine gates" (not shown) put in the I_1-I_2 and I_1-I_3 dot-plots to cut off outlying intensity values. All measured intensities are divided by 1000. Histogram means are: S_1=0.1125, S_3=-0.00014 which should be plugged into Eq. 10s, 11s above for calculation of I_a (Fig. 4s Panel F) and A', the latter necessary for calculation of both the E_0 and E FRET efficiencies (Eq. 12s) and for the calculation of "correlation-based" α via p and q. Additional parameters required for the calculation of the "conventional" α is $M_d = \overline{I_1}$ (5.989) the mean of the I_1 distribution and for the "correlation-based" α is d_0 (6.014), the "square of the width" of distribution I_1 (see also Fig. 2 Panel B).

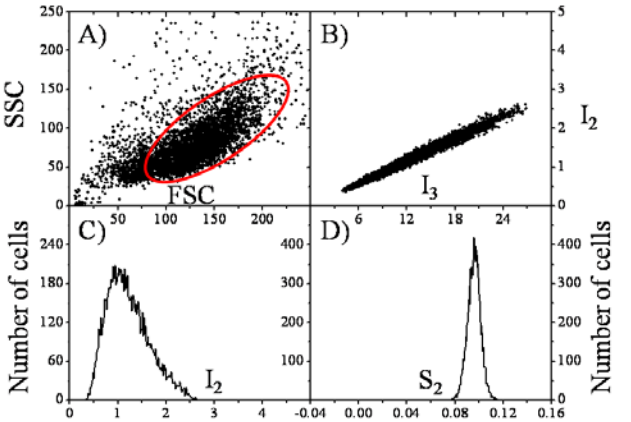

Fig. 3s *Acceptor sample.* The major subpopulation comprising c.a. 80% of the total population of the heterogeneously growing FT cells was separated from the remaining cells and debris based on an "initial gate" (red ellipsis) put in the forward light scatter (FSC)-side scatter (SSC) dot-plot. The I_3-I_2 dot-plot is computed by activating the "initial gate", from which the $S_2=I_2/I_3$ histogram is computed – if necessary, after by activating a new "fine gate" (not shown) put in the I_3-I_2 dot-plot to cut off outlying intensity values. All measured intensities are divided by 1000. Histogram means are: S_2=0.096, which should be plugged into Eqs. 10s, 11s above for calculation of I_a (Fig. 4s Panel F) and A', and $M_a = \overline{I_2}$ (1.2144) the mean of the I_2 distribution for the calculation of "spectral" α (α_0) according to Eq. 2 in the main text

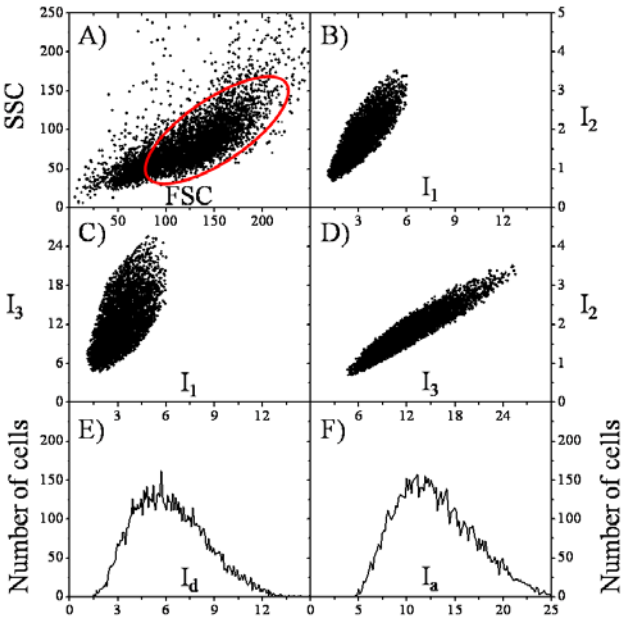

Fig. 4s *Donor+acceptor together (FRET) sample.* The major subpopulation comprising c.a. 80% of the total population of the heterogeneously growing FT cells was separated from the remaining cells and debris based on an "initial gate" (red ellipsis) put in the forward light scatter (FSC)-side scatter (SSC) dot-plot. The I_1-I_2, I_1-I_3 and I_3-I_2 dot-plots are computed by activating the "initial gate", and all the subsequent histograms (A', d', p, q, α, Q, E) are computed from these latter dot-plots – if necessary, after by activating a new "fine gates" (not shown) put in the I_1-I_2, I_1-I_3 and I_3-I_2 dot-plots to cut off outlying intensity values. All measured intensities are divided by 1000. The "spectral α" (α_0) calculated in the conventional way as $\alpha_0 = (\varepsilon_d/\varepsilon_a)\cdot(L_d/L_a)\cdot(B_d/\mathbf{B}_a)\cdot(M_a/M_d) = 4.16$ with L_d=5.0, L_a=1.5 labeling ratios of the donor and acceptor antibodies; the B_d/B_a ratio of the labeled binding sites (in this case unity, being the labeled epitopes two subunits of the same MHCI molecule); the ratio of the absorption coefficients of the donor and acceptor at the wavelength of excitation of the donor $\varepsilon_d/\varepsilon_a$=6.21 ($\varepsilon_d$= 75.2% of ε_{max}=73000 $M^{-1}cm^{-1}$ for Alexa-Fluor-488, ε_a= 7.89% of ε_{max}=112000 $M^{-1}cm^{-1}$ for Alexa-Fluor-546 at 488 nm-excitation); and the ratio M_a/M_d=0.202, where M_d=5.989 is the mean donor intensity in the signal channel I_1 for the sample labeled with only donor (Fig. 2s, Panel D) and M_a=1.2144 is the mean acceptor intensity in the signal channel I_2 for the sample labeled with only acceptor (Fig. 3s, Panel C), after subtracting the corresponding background intensities (Fig. 1s). The "correlation-based α" (0.1) is calculated by using Eqs. 9-12 of the main text, with input parameters d ≈d_0 (6.014) determined from the donor-only sample, and d' (1.0445),p (0.1147), q (0.0194) all determined from the double-labeled sample (for distribution of these quantities, see Fig. 2 Panels B-E). The FRET efficiency as calculated with the "correlation-based" α is E=46.9%, the donor quenching is Q=44.5%, and A'=0.091 (for distributions see Fig. 2 Panels F-H). In the knowledge of distribution of E, the distribution of the unquenched donor intensity of the double-labeled sample I_d (mean value: 3.3258) is calculated according to Eq. 13s (Fig. 4s, Panel E).

Comparative measurements of FRET between epitopes of MHCI at different labeling ratios of mAbs on the surface of FT T-lymphoblast cells: (II.) Alexa-Fluor 488-Alexa-Fluor 546 dye pair

The intra-molecular FRET measurements in the L368 →W6/32 direction pertinent to data of Table 1 in the main text, and both intermolecular FRET measurements (L368-L368, W6/32-W6/32) were repeated on the same cell line with the Alexa-Fluor 488-Alexa-Fluor 546 dye-pair (Table 1s). By inspecting data in Table 1s Part A we can see that the „covariance-based" α-factors are considerably smaller than the conventional α-factors (α_0), leading to E values much larger than E_0, due to the large labeling ratio at the donor side (L_d=5). When compared to the quenching efficiency Q, one accepts E as the true transfer efficiency, being Q equal to E, rather than to E_0, the same result as obtained above with the Alexa-Fluor 546-Alexa-Fluor 647 dye-pair (Table 1 in main text). We remark here also that, although the α-factor depends on the „momentary" optical condition of the cytometer (i.e. on the daily optical alignment), its much smaller value for the Alexa-Fluor 488-Alexa-Fluor 546 dye-pair than for the Alexa-Fluor 546-Alexa-Fluor 647 dye-pair informs us about a much larger difference in sensitivity between the green and red signal channels (α is smaller) than between the two red signal channels (α is larger), as expected.

By inspecting the FRET data pertinent to measurement of homo-associations with the L368 and W6/32 mAbs (Table 1s, Part B), in contrast the much larger α factors obtained with the conventional method (α_0), after correcting the coefficient of the leading quadratic term in Eq. 9 according to Eq. 19 (in main text), essentially the same values were obtained for α_{cubic} as for α_0, implying equal values for E_0 and E.

Table 1s. Conventional and the covariance-based alpha-factors as well as the deduced FRET-efficiencies measured between the β_2m (l.c.) and heavy chain (h.c.) subunits of the MHCI receptor as well as between its heavy chain subunits on the surface of FT T-lymphoblast cells by using Alexa-Fluor 488- and Alexa-Fluor 546-conjugated mAbs

FRET-pairs				Labeling ratio		Alpha-factors			FRET efficiencies (%)		
Donor: Alexa-Fluor 488		Acceptor: Alexa-Fluor 546				Spectral	Covariance-based		Quenching	Quenching & sensitized emission	
mAb	Epitope	mAb	Epitope	L_d	L_a	α_0 [a)]	α [b)]	α_{cubic} [c)]	Q [d)]	E_0 [e)]	E [f)]
Part A											
L368		W6/32				4.16	0.10	-	44	2	39
L368	β_2m	W6/32 low [g)]	MHCI h.c.	5.0	1.5	4.05	0.12	-	35	2	30
L368 low [g)]		W6/32				4.16	0.14	-	45	2	38
Part B											
L368	β_2m	L368	β_2m	5.0	4.7	0.16	0.06	0.16	57	25	25 [h)]
W6/32	MHCI h.c.	W6/32	MHCI h.c.	3.4	1.5	0.57	0.06	0.15	64	8	25 [h)]

[a-i)] With the same meaning of these marks as for Table 1 in main text.

[h)] These values were calculated by using α_{cubic}, the solution of Eq. 20 with m=1.31, b=0.13 (R^2=0.93) obtained by fitting the corresponding Q-Q' plot like that shown in Fig. 3 Panel A.

Comparative measurements of FRET between epitopes of MHCI at different labeling ratios of mAbs on the surface of LS174T-cells

To see the consistency of the „covariance-based" FRET determination at different signal levels – mainly governed by the expression level and degree of homo-association of MHCI in addition to the labeling ratios of the applied mAbs implying altered donor-acceptor ratios and FRET efficiencies – the above experiments on the MHCI proximities were repeated on a different cell line, LS174T colon carcinoma cells. In addition to that the MHCI level on this cell line is c.a. 30% of that on FT cells (29.8±8.9%) the degree of homo-association of MHCI is also considerably smaller. The signal levels also have been modulated by treatments of these cells with the cytokine IFNγ. Interestingly, while IFNγ doubled the expression level of MHCI (190±10%), the degree of its homo-association was reduced, supposedly due to the intercalation of the „intercellular adhesion molecule-1" (ICAM-1) not measured in this study [7]. FRET data on the Alexa-Fluor 546-Alexa-Fluor 647 and on the Alexa-Fluor 546-Cy5 dye-pair are listed in Table 2s. By inspecting Parts A and C it can be seen that the due to the small labeling ratios, the conventional and „covariance-based" α-factors are close to each other, implying a similar relationship between the deduced E_0 and E FRET efficiencies. Moreover in the L368 Fab→W632 intramolecular FRET case, these FRET efficiencies are also close to the quenching efficiency Q, in contrast to the intermolecular cases L368 Fab→

L368 Fab and W6/32→W6/32 when E_0 and E both are much smaller than Q, due to the competition between the dye-targeting mAbs.

When inspecting Part B of Table 2s, the usual behavior can be seen again: Due to the high labeling ratio of the donor-targeting mAb, the conventional „spectral" α-factor is an upper-estimation of the true α, leading to corresponding under-estimation of the true FRET efficiency. However, the covariance-based α-factor gives an acceptable deduced FRET efficiency E also in this case, as proven by its good correspondence with the Q quenching efficiency (Q depending on both competition and FRET, while E_0 and E depending only on FRET).

As to the Alexa-Fluor 546-Cy5 FRET system, by examining Table 2s Part D an interesting observation is that in spite of the large value of the labeling ratio of the acceptor-targeting mAb, the conventional and the „covariance-based" α-factors are practically the same, leading to the same deduced FRET efficiencies. This result implies that at large local concentrations the Cy5 dye behaves differently from the Alexa-Fluor dyes, and/or the dye-conjugation sites for this dye on the W6/32 mAb is such that it does not impairs mAb binding to its epitope on the h.c. subunit of the MHCI receptor.

Table 2s. Conventional and the covariance-based alpha-factors as well as the deduced FRET-efficiencies measured between the β_2m and heavy chain (h.c.) subunits of the MHCI receptor as well as between its heavy chain subunits on the surface of LS174T colorectal carcinoma cells by using Alexa-Fluor 546- and Alexa-Fluor 647- or Cy5-conjugated mAbs.

FRET-pairs				Treat-ment [a]	Labeling ratio		Alpha-factors			FRET efficiencies (%)		
Donor		Acceptor					Spectral	Covariance-based		Quenching		Quenching & sensitized emission
mAb	Epitope	mAb	Epitope		L_d	L_a	α_0 [b]	α [c]	α_{cubic} [d]	Q [e]	E_0 [f]	E [g]
Part A: Alexa-Fluor 546-Alexa-Fluor 647												
L368 Fab	β_2m	W6/32	MHCI h.c.	Cont.	0.8	1.6	0.16	0.15	-	17	18	20
				IFNγ			0.16	0.15	-	17	20	21
Part B: Alexa-Fluor 546-Alexa-Fluor 647												
L368	β_2m	W6/32	MHCI h.c.	Cont.	6.5	2.2	2.42	0.48	-	27	9	34
				IFNγ			2.49	0.55	-	26	8	28
Part C: Alexa-Fluor 546-Alexa-Fluor 647												
L368 Fab	β_2m	L368	β_2m	Cont.	0.8	2.1	0.16	0.05	0.25	63	25	16 [h]
				IFNγ			0.10	0.03	0.14	57	14	11 [h]
Part D: Alexa-Fluor 546-Cy5												
L368 Fab	β_2m	W6/32	MHCI h.c.	Cont.	0.8	4.7	0.16	0.17	-	36	41	40
				IFNγ			0.16	0.19	-	29	39	29

[a] Cells have been treated with IFNγ and at 50 ng/ml concentration, for two days before harvesting.

[b] The conventional (or spectral) alpha-factors (α_0) have been calculated according to Eq. 2 of the main text by using the mean intensities of the samples labeled only with the donor and the acceptor as well as the labeling ratios and absorption coefficients. Due to the 1:1 stoichiometry of the two subunits of the same MHCI molecule, unity was used for the ratio of the labeled receptors (B_d/B_a). All data in this table are representative ones of three different measurements giving similar results, with relative errors <15% (SEM/mean).

[c] Covariance based alpha-factor at the donor side (α) was determined as the mean value of the corresponding cell-by-cell distribution of α obtained as the positive root of the quadratic polynomial in Eq. 9 written for the cell-by-cell distributions of the D, p and q coefficients, examples of which are shown in Fig. 2. In the calculation of the D coefficient in Eq. 9, for the non-competing case of FRET measurement between the β_2m and h.c. subunits, the d value of the FRET sample was approximated by the mean of d_0 distribution of the corresponding single-donor labeled sample.

[d] In the case of FRET indicating homo-association between the MHCI receptors, instead of using d_0 of the single-donor labeled sample, the d value has been approximated from the d' value of the FRET-sample according to Eq. 19 and the positive root of the cubic polynomial in Eq. 20 resulting in a meaningful FRET efficiency (α_{cubic}) was used in the calculation of E. We remark that while the root of the quadratic polynomial of Eq. 9 has been found for each cell and the cell-by-cell distribution of α has been determined, this latter calculation have been carried out only with mean values.

[e] Quenching efficiency (Q) is defined as the relative change in the I_1 donor fluorescence due to the mAb used as acceptor. Mean values of the corresponding cell-by-cell distributions, defined as $Q=1-I_1/I_{1,d}$ where I_1 is intensity of the double-labeled sample and $I_{1,d}$ is the mean intensity of the sample labeled only with the donor, are listed. In the case of competing mAbs for the measurement of MHCI homo-association, it contains also the intensity reducing effect of mAb competition in addition to the effect of FRET.

[f] E_0 has been calculated as the mean of the corresponding cell-by-cell distribution obtained from the A' distribution by using $E_0=A'/(\alpha_0+A')$ (Eq. 12s) with the conventional alpha-factor (α_0) as an input constant.

[g] E has been calculated as the mean of the corresponding cell-by-cell distribution obtained from the A' distribution by using $E=A'/(\alpha+A')$ with the covariance-based alpha-factor (α) as an input constant. These values were calculated by using α_{cubic}, the solution of Eq. 20 with m=3.2, b=0.13 (R^2=0.75) obtained by fitting the corresponding Q-Q' plot like that shown in Fig. 3 Panel A.

Fluorescence lifetime measurement by FLIM

Fluorescence lifetimes of the Alexa-Fluor 488 and Alexa-Fluor 546 dyes conjugated to the L368 and W6/32 mAbs at different labeling ratios have been measured on the cell surface with the FLIM technique. The cell types and processing of the cells have been the same as for flow cytometry. The basic FLIM arrangement – a homodyne detection scheme of phase and modulation lifetimes – has been built around a wide field fluorescence microscope (E-600, Nikon, objective Plan Apo 60x, NA=1.2, water immersion). For the principles and detailed technical description of the homodyne lifetime detection such as camera, image intensifier, signal generators, and signal amplifier we refer to [12]. Briefly: A light emitting diode (LED) (Luxeon III Star, LXHC-LB3C, Lumileds Lighting, US, CA) has been used for illumination (470 nm, 30 mW), the power supply of which was modulated at the same frequency (60 MHz) but at different phases relative to the modulation of the image intensifier. The fluorescence signal channel, corresponding to the I_1 signal of the FCET method, was specified by a 470±15-nm excitation filter (HQ470/30, AF Analysentechnik, Tübingen); a 505DRLP02 dichroic mirror and a 525±15-nm emission filter (525DF30, Omega Optical, Brattleboro, VT). For calibration a standard solution of fluorescein having a 4 nsec-lifetime was used.

Fluorescence lifetime depends on the labeling ratios of mAbs

Seeking for possible reasons for the differences between the conventional (or „spectral") α_0 and the α-factor obtained with the correlation method observed at large dye-per-antibody labeling ratios we measured fluorescence lifetime (proportional with quantum yield) as the function of labeling ratio with the FLIM technique. By applying the phase-modulation method we observed monotonous decreases of phase-lifetime with increasing labeling ratios for the Alexa-Fluor 488-conjugated L368 mAb (a 34.1%-reduction: τ_{phase}=3.93±0.05, 3.25±0.13, 2.59±0.03 ns at labeling ratios L_d=1.5, 1.6, 2.1) and for the Alexa-Fluor 488-conjugated W6/32 mAb (a 28.1%-reduction: τ_{phase}=3.56±0.09, 3.32±0.10, 3.08±0.12, 2.56±0.03 ns at labeling ratios L_d=0.9, 1.0, 2.7, 3.6), n>5 in both cases (Fig. 5s, Panels A, B). The trends can be well fitted with straight lines having slope (s) and intersection (i) s=-1.8, i=6.4 for L368 (R^2=82.5%), and s=-0.3, i=3.8 for W6/32 (R^2=90.3%). In the case of W6/32, with the same labeling ratios the modulation lifetime shows also a similarly decreasing tendency, albeit with a smaller rate than for the phase-lifetime (a 14.1%-reduction: τ_{mod}=3.54±0.04, 3.14±0.06, 3.24±0.05, 3.04±0.03). As a result, the ratio of modulation and phase-lifetimes, a measure of lifetime heterogeneity [12, 13], slightly increases with the labeling ratio (a 20%-increase: τ_{mod}/τ_{phase} =0.99, 0.95, 1.05, 1.19) in accordance with the view that the number of non-emitting, dark complexes and consequently, the rate of FRET towards these complexes may

increase. Similar decreases in lifetime but with much larger magnitudes were observed for the Alexa-Fluor 546-conjugated L368 mAb (a 59.7%-decrease for the phase-lifetime: τ_{phase}=2.01±0.03, 1.45±0.04, 0.81±0.09, and a 53.3%-decrease for the modulation-lifetime: τ_{mod}=3.19±0.01, 2.48±0.01, 1.49±0.03 at L_a=1.2, 2.7, 3.5), and only a modest (15%) increase in the lifetime ratio similarly to the Alexa-Fluor 488 (Fig. 5s, Panel C). However, when the absolute values of lifetime ratios are compared, these are much larger for Alexa-Fluor 546 than for Alexa-Fluor 488 (1.6 vs. 1.0 at the smallest labeling ratios, Fig. 5 Panels B, C), implying a much larger tendency for complex formation for Alexa-Fluor 546.

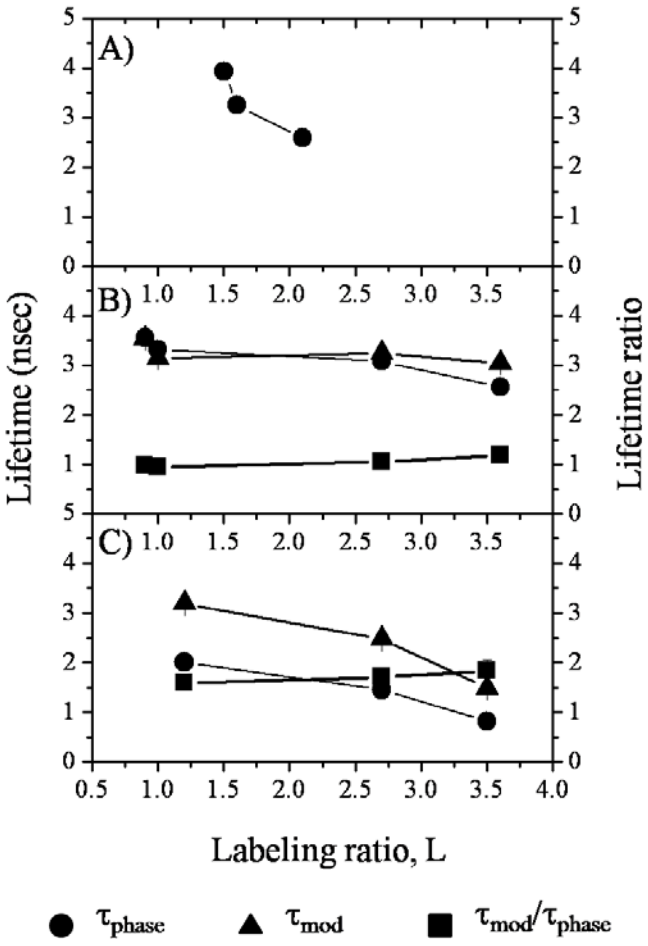

Fig. 5s *Fluorescence lifetimes of dye-conjugated mAbs as the function of labeling ratio.* Phase and modulation lifetimes (τ_{phase}, τ_{mod}) and their ratio (τ_{mod}/τ_{phase}) as measured with the FLIM technique. While the phase and modulation lifetimes monotonously decrease, their ratio increases with increasing labeling ratio of the dye-targeting mAbs, implying increasing interaction between the dyes with the increasing local concentration. The interaction is largely mediated by homo-FRET being the critical Förster-distance comparable to the size of mAbs: $R_{0,\ Förster}$~4 nm vs. ~3.5 nm smaller and ~6.5 nm larger diameter of an Fab-fragment as a rotational ellipsoid [14]. The increasing lifetime ratio indicates increasing lifetime heterogeneity in accordance with the increased number of different dye microenvironments. Panel A: Alexa-Fluor 488-conjugated L368, Panel B: Alexa-Fluor 488-conjugated W6/32, Panel C: Alexa-Fluor 546-conjugated W6/32. Error bounds are within the size of symbols.

Overview of the correlation method

The point in the newly developed method is that besides the conventional system of equations (Eqs. 1s-3s in *Supplement*) characterizing the FRET-system, based on „suitably defined" variance and covariance terms calculated from intensities of the donor-only and FRET samples (labeled with only donor, and with both donor and acceptor, respectively), a quadratic equation (Eq. 9) can be set up for the α factor whose positive root serves as the accepted value of α (see Fig. 1 for a summary of the new method). Advantageous properties of the quadratic equation are that: (i) The positive root is always existing. (ii) Because the covariance and variance are averages of the corresponding fluctuation products and squares, an analogue quadratic equation can be formulated also for the corresponding fluctuation square and product terms, which by the fact that they can be determined on a cell-by-cell

basis, enables the determination of α factor for each individual cell, i.e. it enables the determination of the cell-by-cell distribution of α factor (Fig. 2, Panel E). (iii) Although essentially two samples are needed for the determination of the α factor (notwithstanding now the determination of the spillage factors), the donor-only (for d_0) and the FRET samples (for d'), it can be shown that this rigor can be significantly relaxed if the variation of donor-moment is known as the function of the donor intensity (Q'-Q plots, Fig. 3 Panel A), when the α factor is determined on the very double-labeled sample from which the FRET efficiency is eventually calculated (by Eq. 20). (iv) By approximating d with d_0 gives the true value for α in the absence of any competition of the dye-targeting ligands (or other non-FRET interaction), α is underestimated, and consequently E is upper-estimated in the presence of it.

Comparative measurements of FRET at different labeling ratios of mAbs reveal differences in the conventional and covariance-based FRET determinations

In the framework of the FCET-method, as it has been originally worked out by Trón *et al.* [9, 10] the α-factor is determined based on the mean intensities of the donor- and acceptor-only samples in the knowledge the relative absorption coefficient of the donor and the acceptor ($\varepsilon_d/\varepsilon_a$) at the excitation wavelength of the donor, the labeling ratios of the donor- and acceptor-conjugated ligands (L_d, L_a), and the numbers of the labeled receptors (B_d, B_a) (Eq. 2). According to the correlation-based method, the α-factor is determined by the positive root of Eq. 9 which is simple quadratic in those cases when the coefficient of the quadratic term (D) can be calculated with the intensity moment of the donor-only sample (d_0) as an input parameter ($D=d_0-d'$), i.e. as far as there is no steric interaction between the labels.

When comparing the α-factors determined in the two ways obtained in measurements of FRET between the epitopes of MHCI (Tables 1, 2, 1s), we can recognize that one important factor behind their possible deviation is the labeling ratio (L_d, L_a) of the used dye-conjugated ligands. While for small labeling ratios around unity (in the range 0.5-2), good correspondence can be found between the two kinds of α, at large ones (>3) substantial deviations may occur, but not necessarily, possibly depending on the position of dye-conjugation sites on the ligands. Alternatively two errors, one in the numerator and another in the denominator, committed in the determination of the labeling ratios (L_d, L_a) and/or binding sites (B_d, B_a) could cancel each other in Eq. 15. Based on published data of others [15-20], as well as our own experience there are two main factors governing brightness (effective fluorescence) of dye-conjugated ligands: (i) spectral interactions of the spatially confined dyes, facilitated by the large local concentrations due to the small ligand size – e.g. 1 dye in an area of an effective diameter of an Fab fragment (5 nm) means 85 mM local concentration, and (ii) impaired binding of ligand to its receptor due to shielding of binding sites by the dressing dyes.

(i) As to the spectral interactions, the large local concentrations can favor the formation of dark complexes with their absorption spectra shifted towards larger wavelengths, favoring hetero-FRET from monomers towards complexes, which is accelerated by possible homo-FRET between the monomers in close proximity (FRET cascade), being the characteristic Förster distance ~ 4nm, comparable to the radius of an mAb ~6.5 nm [14]. This result in acting of dark complexes as traps for the excitation energy [20], manifested in a decrease in quantum yield, or equivalently in the „effective dye-per-protein labeling ratio". This physical picture is corroborated by the fact that fluorescence anisotropy of these mAbs decrease with increasing labeling ratio [21]. Alternatively, this same phenomenon can also be treated in terms of reduced lifetime, being lifetime proportional to the quantum yield, as observed by us with fluorescence lifetime imaging microscopy (FLIM) (Fig. 5s). Physically this implies that, the error is committed by not using the effective absorption coefficients

corresponding to the number of FRET events. While on the donor side the absorption is over-estimated, on the acceptor side under-estimated.

Mathematically the reason of the error is in assuming linear relationship between fluorescence and the labeling ratio in Eq. 2 [15]. Although in some cases (e.g. mAbs) there is a possibility to correct mathematically this error by using the appropriate functional dependence after suitable calibration of the ligand fluorescence (measurements of quantum yields and lifetimes as the function of labeling ratio on the cell surface) we favor our method using the in-situ intensity correlations on the cell surface, because quantum yield calibration is generally not easily done and lifetime measurements are not readily available on the surface of living cells.

(ii) The other possible candidate behind the error could be the effect of shielding of binding sites (directed towards the receptors) on the ligands by the conjugated dyes, leading to the reduction in the effective labeling ratio of the ligands actually bound to the receptors as compared to the unbound ligands – a kind of „sieving property" in terms of the number of the effectively bound dyes. That this „sieving property" may operate at large dye-per-protein labeling ratios is indicated by our experience that the intensity reduction of the bound ligands maybe larger than the reduction in effective lifetime.

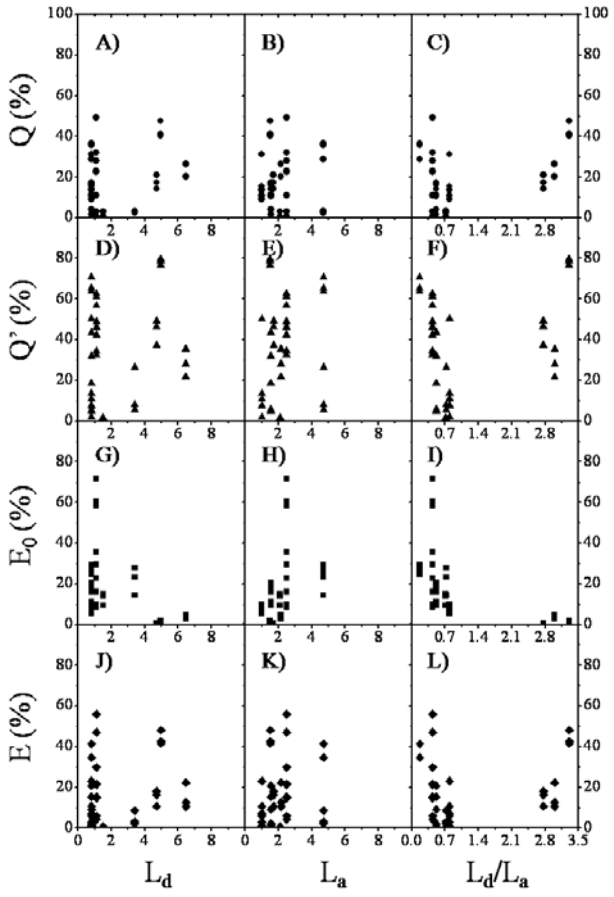

Fig. 6s *Dependence of FRET indices on the labeling ratios of mAbs.* While the trends of all FRET-indices are similar at small donor labeling ratios (<4) and small L_d/L_a values (<1.4), the trend of E_0 (Panels G, H, I) deviates from those of E, Q, and Q' towards small values at large donor labeling ratios (>4) and large L_d/L_a values (>1.4), in accordance with the observed bad correlations of E_0 with E, Q and Q' (Fig. 3 Panels B, C, E in the main text). While all FRET indices with the exception of E_0 stay constant with the donor labeling ratio L_d (1st column), they all increase with the acceptor labeling ratio L_a (2nd column). This observation seems to be corroborated by that increasing L_d/L_a reduces FRET (3rd column).

Estimating intensity variation of d from a single cell-by-cell distribution of the I_1 donor intensity

For determining the functional form of the dependence of Q' on Q, measurements of I_1 on at least 2-3 different donor samples are needed. However there could occur practical cases (e.g. rare genetically engineered protein samples) when only a single donor sample is available. For handling these cases the question arises whether the intensity variation of the second moment of the intensity distribution (i.e. the dependence of the distribution width on the mean intensity) can be forecasted by using the intensity distribution of a single sample either singly donor labeled, or doubly labeled with both donor and acceptor.

According to our experience, an approximation can be obtained by successive gating on the I_2 intensity axes of the I_1-I_2 correlation dot-plots. In this procedure the $I_{2,min}$- $I_{2,max}$ range of the I_2 intensity is divided into a number of intervals (n=20 is adequate in practice), such a way that each interval has the same $I_{2,min}$ as left endpoint, and the right endpoint is successively increases with the same width of w= ($I_{2,max}$- $I_{2,min}$)/n. This way a series of increasing intervals is obtained such a way that each interval contains the previous one as a subset and the last interval coincides with the total $I_{2,min}$-$I_{2,max}$ interval itself. The interval series defined on the I_2 axis fixes a corresponding series of distribution on the I_1 axis, with the largest one the distribution I_2 itself („conditional distributions", where instead of I_2 could also be I_3, FSC, SSC). By plotting the individual moments („conditional variances") [22] of the members of this series as the function of the respective mean values („conditional means") a curve is obtained which is characteristic to the intensity distribution. By fitting this curve with an appropriate function („trend line") an analytic form can be obtained which can be used for estimating the unknown d value from the measured d' and A'. According to our experience the best fit having a correlation coefficient close to unity is an exponential of the form

$$d = p_{1,fit} \cdot e^{p_{2,fit} \cdot I_d}, \tag{14s}$$

with limiting values d($I_d = \overline{I_1}$)=d_0 on the donor-only sample, and d($I_d = \overline{I_1}$)=d' on the double-labeled sample (where $\overline{I_1}$ now designates the right end-point of the I_d values, which is the mean of the I_1 distribution). Because FRET generally means only a modest perturbation of the I_1 intensity distribution, the „work function" in Eq. 14s can equally well be applied for both the singly labeled and doubly labeled samples with approximately the same fitting constants. For the sake of comparison with the previous procedure of fitting the Q'-Q curves, a linearized version of the exponential in Eq. 14s can be obtained by giving the equation of the tangent line at the right end-point (i.e. at $\overline{I_1}$):

$$d = m' \cdot I_d + b', \tag{15s}$$

with

$$m' = p_{1,fit} \cdot p_{2,fit} \cdot e^{p_{2,fit} \cdot \overline{I_1}}, \tag{16s}$$

$$b' = p_{1,fit} \cdot e^{p_{2,fit} \cdot \overline{I_1}} - m' \cdot \overline{I_1}. \tag{17s}$$

That the two procedures (fitting of the Q' vs. Q curve in Eq. 18 and the fitting of the exponential in Eq. 14s) lead to the same results is also proved by the fact that the coefficients of the trend line in Eq. 18 are almost the same as those in Eq. 14s. After fixing the coefficients of the trend line in Eq. 14s and expressing I_d based on Eq. 5 as the function of A' and α, d can

be expressed as the function of A' and α and plugged into Eq. 9 via Eq. 10, thereby arriving at the following transcendental equation for α:

$$\left[p_{1,fit}\cdot e^{p_{2,fit}\cdot\overline{I_1}\cdot\left(1+\overline{A'}/\alpha\right)}-d'\right]\cdot\alpha^2-2\cdot p\cdot\alpha-q=0, \tag{18s}$$

where the upper bars designate averaging. The „relevant" roots (positive and „large enough" for producing E<1) of Eq. 18s serve as α. When d is expressed with A' and α via the approximating tangent line of Eq. 14s, Eq. 18s will reduce to a cubic polynomial, like in the case of Eq. 18 as already discussed above.

As to the experimental results, in the case of the Alexa-Fluor 546-L368-Alexa-Fluor 647-W6/32 FRET-pairs of Table 1 Panel A: α=0.38, 0.24, 0.50 for each entry, respectively, with fitting parameters $p_{1,fit}$=0.059, $p_{2,fit}$=2.215 (R^2=0.98), for the L368-L368 and W6/32-W6/32 FRET-pairs of Table 1 Panel C: α=0.18, 0.20, respectively, with fitting parameters $p_{1,fit}$=0.059, $p_{2,fit}$=2.215 (R^2=0.95), and $p_{1,fit}$=0.21, $p_{2,fit}$=0.255 (R^2=0.96). In the case of the Alexa-Fluor 488-L368-Alexa-Fluor 546-W6/32 FRET-pairs of Table 2 Panel A: α=0.09, 0.10, 0.15 with the fitting parameters $p_{1,fit}$=0.023, $p_{2,fit}$=0.930 (R^2=0.99).

Estimating d by using Eq. 2, a hybrid approach, when the labeling ratios are small

In this case we assume that Eq. 2 for the α is strictly valid (as is the case for labeling ratios around unity), and that the donor-to-acceptor concentration ratio (B_d/B_a) is the same and known value for each individual cell (or pixel). By isolating the ρ "absorbance ratio" in Eq. 2 as

$$\rho=\frac{\varepsilon_d\cdot L_d\cdot B_d}{\varepsilon_a\cdot L_a\cdot B_a}, \tag{19s}$$

and replacing M_a and M_d with $S_2\cdot I_a$ and I_d of the double-labeled sample, respectively, we arrive at an alternative form of Eq. 2, which is applicable on a cell-by-cell basis:

$$\alpha=\rho\cdot S_2\cdot I_a/I_d\,. \tag{20s}$$

The use of Eq. 20s is in that it connects the unknown unperturbed donor moment (d) introduced in Eq. 7 to the acceptor moment

$$d_a=\left(I_a,I_a\right), \tag{21s}$$

which is measurable also on the FRET sample (for I_a see Eq. 11s):

$$d=\left(\rho\cdot S_2/\alpha\right)^2\cdot d_a\,. \tag{22s}$$

This form of d – via also Eq. 10 for D – results in an alternative form of Eq. 9 defining α:

$$d'\cdot\alpha^2+2\cdot p\cdot\alpha+\left[q-\left(\rho\cdot S_2\right)^2\cdot d_a\right]=0\,, \tag{23s}$$

which can be used for determining α on a cell-by-cell basis as far as ρ is a known constant value for each cell – e.g. in the case of two subunits of the same MHCI receptor, or when homo-association is measured. Expanded form of the constant term of Eq. 23s as the function of the moments of I_1, I_2 and I_3 can be obtained from the expanded form of q (Eq. 14) by the following replacements of (I_2, I_2), (I_2, I_3), and (I_3, I_3) via Eq. 11s for I_a:

$$\left(I_2,I_2\right)\rightarrow\left[1-\left(\rho\cdot S_2\cdot S_3/S_1\right)^2\right]\cdot\left(I_2,I_2\right), \tag{24s}$$

$$(I_2, I_3) \to \left[1 - \rho^2 \cdot S_2 \cdot S_3 / S_1\right] \cdot (I_2, I_3), \tag{25s}$$

$$(I_3, I_3) \to \left(1 - \rho^2\right) \cdot (I_2, I_3). \tag{26s}$$

Acceptor moments: alternative deduction of Eq. 9 for α and entropic interpretation of the moments

Further insight into the physical meaning of the coefficients D, p, and q for the quadratic polynom defining α (Eq. 9) can be gained by taking into account also the moments of acceptor and by taking the sum of the donor and acceptor signals as a whole. The idea is that although FRET reduces donor signal and enhances acceptor signal separately in the donor and acceptor channels, and consequently changes the corresponding individual moments similarly, it does not affect the sum of the donor and acceptor signals and the moment of the sum. If the donor energy is designated by ξ, acceptor energy by ψ, and the transferred energy by ζ, then $(\xi + \psi)_{no\ FRET} = \left[(\xi - \zeta) + (\psi + \zeta)\right]_{with\ FRET}$, so the moments of the total signal before and after FRET should be the same. By going over to the language of moments and applying Eqs. 1s, 2s of the *Supplement*:

$$\begin{aligned} &(\alpha \cdot I_d + I_a \cdot S_2,\ \alpha \cdot I_d + I_a \cdot S_2)_{no\,FRET} = \\ &= (\alpha \cdot I_d \cdot (1 - E) + I_a \cdot S_2 + \alpha \cdot I_d \cdot E,\ \alpha \cdot I_d \cdot (1 - E) + I_a \cdot S_2 + \alpha \cdot I_d \cdot E)_{with\,FRET}. \end{aligned} \tag{27s}$$

By replacing $I_d \cdot (1 - E)$ with I_1 (Eq. 1s), and by replacing $\alpha \cdot I_d \cdot E$ with $I_1 \cdot A'$ (deducible from Eqs. 12s, 13s) :

$$\begin{aligned} &(\alpha \cdot I_d + I_a \cdot S_2,\ \alpha \cdot I_d + I_a \cdot S_2)_{no\,FRET} = \\ &= (\alpha \cdot I_1 + I_a \cdot S_2 + I_1 \cdot A',\ \alpha \cdot I_1 + I_a \cdot S_2 + I_1 \cdot A')_{with\,FRET}. \end{aligned} \tag{28s}$$

Although the acceptor channel I_2 contains as a portion the overspill of the donor into this channel, we left out from the expression of the total signal, to contain only the real contributions of the donor and the acceptor. If now the acceptor moment without FRET and with FRET is designated by d_a' and d_a'' and defined with I_a (Eq. 11s) and A' as follows:

$$d'_a = (S_2 \cdot I_a, S_2 \cdot I_a), \tag{29s}$$

$$d''_a = (I_a \cdot S_2 + I_1 \cdot A', I_a \cdot S_2 + I_1 \cdot A'), \tag{30s}$$

Then from Eq. 28s the difference of donor moments without and with FRET (which is the leading term of Eq. 9) can be expressed in terms of the acceptor moments:

$$(d - d') \cdot \alpha^2 = d''_a - d'_a + 2 \cdot \left[\alpha \cdot (I_1, I_1 \cdot A') - S_2 \cdot (I_a, I_1 \cdot A')\right]. \tag{31s}$$

After expending d_a'' in Eq. 30s, the d_a''-d_a' difference in Eq. 31s can be replaced by

$$d''_a - d'_a = 2 \cdot S_2 \cdot (I_a, I_1 \cdot A') + (I_1 \cdot A', I_1 \cdot A'), \tag{32s}$$

arriving at

$$(d - d') \cdot \alpha^2 = 2 \cdot (I_1, I_1 \cdot A') \cdot \alpha + (I_1 \cdot A', I_1 \cdot A'), \tag{33s}$$

which is just Eq. 9, the quadratic equation already deduced for α determination, with $D = d - d'$, $p = (I_1, I_1 \cdot A')$, $q = (I_1 \cdot A', I_1 \cdot A')$. The significance of this formalism is not only in that it enabled a second way of deduction of Eq. 9, but also that it enables us to attach physical interpretations to the meaning of the donor and acceptor moment differences and covariances. (i) Based on Eq. 33s the reduction in donor moment has two sources: the first term is the modulation of the remaining donor signal (I_1) by the transferred energy ($I_1 \cdot A'$), and the second term is the moment of the transferred energy. The interpretation of the first term as a kind of modulation is facilitated by the application of a general formula (according to Huber) [23] enabling us to convert covariances into the difference in two variances:

$$(I_1, I_1 \cdot A') = [(I_1 + I_1 \cdot A', I_1 + I_1 \cdot A') - (I_1 - I_1 \cdot A', I_1 - I_1 \cdot A')]/4. \quad (34s)$$

(ii) Similarly for the acceptor, the 1st term on the right side of Eq. 32s is the modulation of the acceptor signal (I_a) by the transferred energy ($I_1 \cdot A'$), and the 2nd term is the moment of the transferred energy. (iii) Eq. 31s expresses the counterintuitive observation that the reduction in donor moment in general is not compensated by the increase in acceptor moment. The difference depends on α, and will be zero for a special α when

$$\alpha = S_2 \cdot (I_a, I_1 \cdot A') / (I_1, I_1 \cdot A'). \quad (35s)$$

Eq. 31s also informs us that the difference between the changes of the donor and acceptor moments can be attributed to the different degree of modulations of the donor and acceptor signals caused by the transferred energy, and when this modulation is the same the difference cancels (Eq. 35s). Eq. 35s has an important practical consequence: α depends on the optical conditions of the measurement and can be changed with the optical conditions at custom. For α values fulfilling Eq. 35s

$$\alpha = \sqrt{(d_a'' - d_a') / (d - d')} \quad (36s)$$

is also fulfilled. As to the sign of the difference in Eq. 31s, it can be either positive or negative, but when S_2 (the ratio of acceptor's excitabilities at the acceptor and donor excitation wavelength) is adjusted experimentally to zero, then the sign is definitely positive, meaning that the expression of Eq. 36s gives an under estimation for the real α in these cases. It is also can be seen, that for weak FRET processes (A'≈0) this difference can be taken as zero, and Eq. 36s approximately equals to the real α irrespective of the value of S_2. Changes of donor and acceptor moments can also be interpreted as corresponding changes in entropy or information content of the signals (according to Kullback) [24]. In the framework of the entropy interpretation, Eq. 31s means that the reduction in entropy of the donor signal is not compensated for by an equal increase of entropy of the acceptor signal, there is a net entropy production (2nd term in Eq. 31s) responsible for the mixing of transferred energy with the donor and acceptor signals (reminiscent of „mixing entropy" of thermodynamics).

Error estimation of α determined from the quadratic equation (Eq. 9)

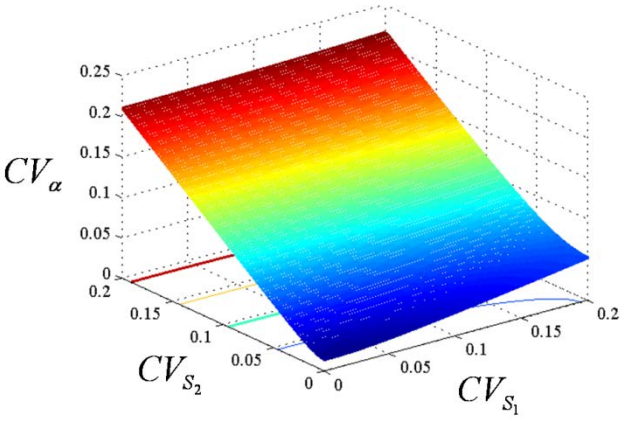

Fig. 7s *Dependence of CV_α on CV_{S1} and CV_{S2}.* Error estimation has been done with the Gaussian law of error propagation based on Eqs. 9, 13, 14 in the main text. The error surface belongs to data of the 3rd row of Table 2, Part A: Alexa-Fluor 488-conjugated L368 "low" as donor+Alexa-Fluor 546-conjugated W6/32 as acceptor (α=0.135). According to Eq. 9 error of α can be decomposed to errors in the D, p and q quantities. While D does not depend on the S_1 and S_2 spillage factors, p and q do, as shown by Eqs. 13, 14. The effect of the S_3 factor has not been taken into account being this factor negligibly small in our case (S_3=1.5x10^{-4}). Coefficient of variation square of α has been estimated with coefficient of variation squares for D, p and q based on Eq. 9:

$$CV_\alpha^2 = \left[\tilde{p}^2 \cdot CV_p^2 + 1/4 \cdot \tilde{q}^2 \Big/ \left(\sqrt{\tilde{p}^2 + \tilde{q}} + \tilde{p}\right)^2 \cdot CV_q^2\right] \Big/ \left(\tilde{p}^2 + \tilde{q}\right) + \left(2 \cdot p + q/\alpha\right)^2 \cdot CV_D^2, \quad (37s)$$

with $\tilde{p} \equiv p/D$, $\tilde{q} \equiv q/D$. Coefficient of variation squares for p and q has been computed based on Eqs. 13, 14:

$$CV_p^2 = \left(S_1^2 \cdot d'^2 \cdot CV_{S_1}^2 + S_2^2 \cdot d_{13}^2 \cdot CV_{S_2}^2\right) \Big/ p^2, \quad (38s)$$

$$CV_q^2 = 4 \cdot \left[S_1^2 \cdot \left(S_1 \cdot d' + S_2 \cdot d_{13} - d_{12}\right)^2 \cdot CV_{S_1}^2 + S_2^2 \cdot \left(S_2 \cdot d_3 + S_1 \cdot d_{13} - d_{23}\right)^2 \cdot CV_{S_2}^2\right] \Big/ q^2. \quad (39s)$$

With the definitions: $d' \equiv (I_1, I_1)$, $d_2 \equiv (I_2, I_2)$, $d_3 \equiv (I_3, I_3)$, $d_{ij} \equiv (I_i, I_j)$, i, j=1, 2, 3. Used constants: S_1=0.1143, S_2=0.096, D=1.2406 (D and d's are multiplied by 10^{-6}), p=0.04, q=0.01, d'=0.338, d_2=0.248, d_3=16.616, d_{12}=0.227, d_{13}=1.549. d_{23}=1.969, CV_D=0.1.

It can be seen from the error surface that at the experienced CV-s of the spillage factors (CV_{S1}=0.1095, CV_{S2}=0.0558) CV_α remains around 0.05.

Stability of α determined from the cubic equation (Eq. 20)

The sensitivity of the coefficients of the cubic equation Eq. 20 on changes in the S_1 and S_2 spillage factors has been examined by applying the Gaussian law of error propagation on the coefficients p_0, p_1, and p_2 (Eqs. 22-24, 40s-55s). (p_3 does not depend on S_1 and S_2.) These coefficients has been expressed as explicit functions of S_1 and S_2 based of the dependence of A', p, q on S_1 and S_2 as expressed by Eqs. 10s, 13, 14 (Eqs. 40s-55s). According to Figs. 8s-10s below, a 0.023 and 0.066 coefficients of variation of S_1 and S_2 cause 0.48, 0.28 and 0.2 coefficients of variation in p_0, p_1, and p_2, respectively. To see the degree of tolerance of α, a 10, 14, 24, and 10 %-change (the last three are half of those caused by the variation of S_1 and S_2) for each one of the p0-p3 coefficients, respectively – while the others has been kept constant – caused only a 4-13 % change in α. When all the 4 coefficients has been shifted by these %-values in either the increasing or the decreasing direction, only a ~10 % change in α could be elicited demonstrating a degree of resistance of α against changes in the coefficients p0-p3. Although these results have been obtained for the Alexa-Fluor 546-W6/32+Alexa-Fluor 647-W6/32 donor-acceptor pair, similar results could be calculated also for the L368-L368 mAb pair with the same dyes – the 7th row of Table 1 – and for the Alexa-Fluor 488-Alexa-Fluor 546 dye pair with both types of mAb – the 7th and 8th rows of Table 2.

Fig. 8s *Dependence of CV_{p0} on CV_{S1} and CV_{S2} (Eq. 53s).* The error surface has been calculated for the case of Alexa-Fluor 488-W6/32+Alexa-Fluor 546-W6/32 donor-acceptor pair – the 8th row of Table 1 – having parameter values: α_{cubic}=0.139, p_3=-19.574, p_2=-2.455, p_1=0.470, p_0=0.034, S_1=0.188, S_2=0.096, CV_{S1}=0.023, CV_{S2}=0.066.

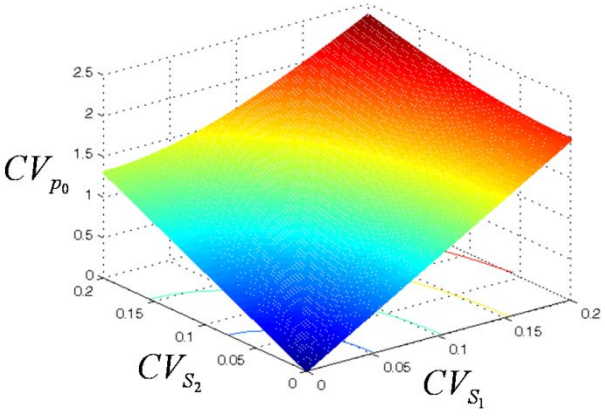

Fig. 9s *Dependence of CV_{p1} on CV_{S1} and CV_{S2} (Eq. 54s).* Sample and parameters are as above.

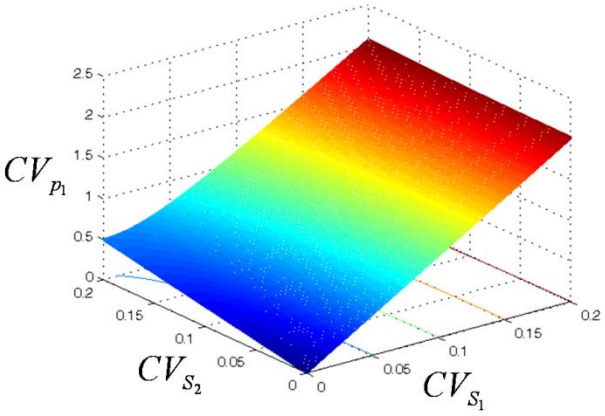

Fig. 10s *Dependence of CV_{p2} on CV_{S1} and CV_{S2} (Eq. 55s).* Sample and parameters are as above.

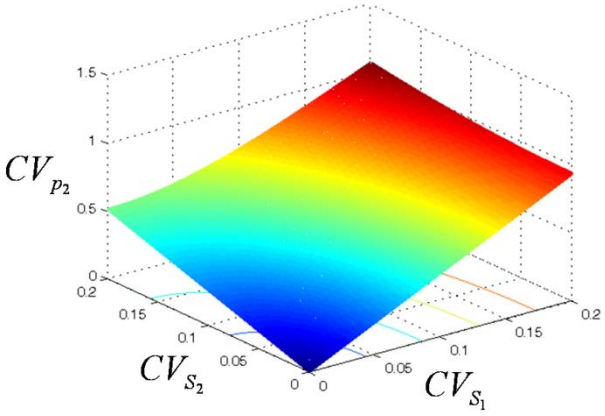

Formulae for the sensitivity of the cubic equation

For computing partial derivatives of the p_0, p_1, and p_2 according to the S_1 and S_2 spillage factors, first explicit forms of the p, q and A' quantities as functions of S_1 and S_2 are deduced from Eqs. 13, 14, and 10s:

$$p = d_{12} - S_1 \cdot d' - S_2 \cdot d_{13}, \tag{40s}$$

$$q = d_2 - 2 \cdot S_1 \cdot d_{12} - 2 \cdot S_2 \cdot d_{23} + 2 \cdot S_1 \cdot S_2 \cdot d_{13} + S_1^2 \cdot d' + S_2^2 \cdot d_3, \tag{41s}$$

$$A' = i_2 - S_2 \cdot i_3 - S_1, \tag{42s}$$

with the same definitions of the d-s as after Eq. 39s above, and with $i_2=I_2/I_1$, and $i_3=I_3/I_1$. According to Eqs. 22-24, the following partial derivatives are necessary for the calculation of errors: For p_0,

$$\partial A'{\cdot}q/\partial S_1 = -\left(2\cdot i_2\cdot d_{12}+d_2\right)+2\cdot S_1\cdot\left(i_2\cdot d'+2\cdot d_{12}\right)+2\cdot S_2\cdot\left(i_2\cdot d_{13}+i_3\cdot d_{12}+d_{23}\right) \quad (43s)$$
$$-2\cdot S_1\cdot S_2\left(i_3\cdot d'+2\cdot d_{13}\right)-3\cdot S_1^2\cdot d'-S_2^2\cdot\left(2\cdot i_3\cdot d_{13}+d_3\right),$$

$$\partial A'{\cdot}q/\partial S_2 = -\left(2\cdot i_2\cdot d_{23}+i_3\cdot d_2\right)+2\cdot S_1\cdot\left(i_2\cdot d_{13}+i_3\cdot d_{12}+d_{23}\right)+ \quad (44s)$$
$$2\cdot S_2\cdot\left(i_2\cdot d_3+2\cdot i_3\cdot d_{23}\right)-2\cdot S_1\cdot S_2\left(2\cdot i_3\cdot d_{13}+d_3\right)-S_1^2\cdot\left(i_3\cdot d'+2\cdot d_{13}\right)-3\cdot S_2^2\cdot i_3\cdot d_3.$$

For p_1:

$$\partial A'{\cdot}p/\partial S_1 = -\left(i_2\cdot d'+d_{12}\right)+2\cdot S_1\cdot d'+S_2\cdot\left(i_3\cdot d'+d_{13}\right), \quad (45s)$$

$$\partial A'{\cdot}p/\partial S_2 = -\left(i_2\cdot d_{13}+i_3\cdot d_{12}\right)+S_1\cdot\left(i_3\cdot d'+d_{13}\right)+2\cdot S_2\cdot i_3\cdot d_{13}, \quad (46s)$$

$$\partial q/\partial S_1 = -2\cdot d_{12}+2\cdot S_1\cdot d'+2\cdot S_2\cdot d_{13}, \quad (47s)$$

$$\partial q/\partial S_2 = -2\cdot d_{23}+2\cdot S_1\cdot d_{13}+2\cdot S_2\cdot d_3, \quad (48s)$$

$$\partial p_1/\partial S_1 = -2\cdot\left(1-m-b\right)\cdot\partial A'\cdot p/\partial S_1-\left(1-b\right)\cdot\partial q/\partial S_1, \quad (49s)$$

$$\partial p_1/\partial S_2 = -2\cdot\left(1-m-b\right)\cdot\partial A'\cdot p/\partial S_2-\left(1-b\right)\cdot\partial q/\partial S_2. \quad (50s)$$

For p_2:

$$\partial p_2/\partial S_1 = -\left(m-2+3\cdot b\right)\cdot d', \quad (51s)$$

$$\partial p_2/\partial S_2 = -\left(m+b\right)\cdot i_3\cdot d'+2\cdot\left(1-b\right)\cdot d_{13}. \quad (52s)$$

With these partial derivatives the CV^2-s are the following:

$$CV_{p_0}^2 = \left(1-m-b\right)\cdot\left[\left(\partial A'{\cdot}q/\partial S_1\right)^2\cdot S_1^2\cdot CV_{S_1}^2+\left(\partial A'{\cdot}q/\partial S_2\right)^2\cdot S_2^2\cdot CV_{S_2}^2\right]/p_0^2, \quad (53s)$$

$$CV_{p_1}^2 = \left[\left(\partial p_1/\partial S_1\right)^2\cdot S_1^2\cdot CV_{S_1}^2+\left(\partial p_1/\partial S_2\right)^2\cdot S_2^2\cdot CV_{S_2}^2\right]/p_1^2, \quad (54s)$$

$$CV_{p_2}^2 = \left[\left(\partial p_2/\partial S_1\right)^2\cdot S_1^2\cdot CV_{S_1}^2+\left(\partial p_2/\partial S_2\right)^2\cdot S_2^2\cdot CV_{S_2}^2\right]/p_2^2. \quad (55s)$$

Supporting references

1. Hori, T., T. Uchiyama, M. Tsudo, H. Umadome, H. Ohno, S. Fukuhara, K. Kita, and H. Uchino. 1987. Establishment of an interleukin 2-dependent human T cell line from a patient with T cell chronic lymphocytic leukemia who is not infected with human T cell leukemia/lymphoma virus. *Blood* 70: 1069–1072.
2. Szöllősi, J., V. Hořejší, L. Bene, P. Angelisová, and S. Damjanovich. 1996. Supramolecular complexes of MHC class I, MHC class II, CD20, and tetraspan molecules (CD53, CD81, and CD82) at the surface of a B cell line JY. *J. Immunol.* 157: 2939-2946.

3. Tanabe, M., M. Sekimata, S. Ferrone, and M. Takiguchi. 1992. Structural and functional analysis of monomorphic determinants recognized by monoclonal antibodies reacting with HLA class I alpha 3 domain. *J. Immunol.* 148: 3202-3209.
4. Szöllősi, J., S. Damjanovich, M. Balázs, P. Nagy, L. Trón, M. J. Fulwyler, and F. M. Brodsky. 1989. Physical association between MHC class I and class II molecules detected on the cell surface by flow cytometric energy transfer. *J. Immunol.* 143: 208-213.
5. Edidin, M., and T. Wei. 1982. Lateral diffusion of H-2 antigens on mouse fibroblasts. *J. Cell Biol.* 95: 458-462.
6. Bene, L., M. Balázs, J. Matkó, J. Most, M. P. Dierich, J. Szöllősi, and S. Damjanovich. 1994. Lateral organization of the ICAM-1 molecule at the surface of human lymphoblasts: a possible model for its codistribution with the IL-2 receptor, class I and class II HLA molecules. *Eur. J. Immunol.* 24: 2115-2123.
7. Bacsó, Z., L. Bene, L. Damjanovich, and S. Damjanovich. 2002. IFN-γ rearranges membrane topography of MHC-I and ICAM-1 in colon carcinoma cells. *Biochem. Biophys. Res. Commun.* 290: 635-64.
8. Bene, L., Z. Kanyári, A. Bodnár, J. Kappelmayer, T. A. Waldmann, G. Vámosi, and L. Damjanovich. 2007. Colorectal carcinoma rearranges cell surface protein topology and density in $CD4^+$ T cells. *Biochem. Biophys. Res. Commun.* 361: 202-207.
9. Trón, L., J. Szöllősi , S. Damjanovich, S. H. Helliwell, D. J. Arndt-Jovin, and T. M. Jovin. 1984. Flow cytometric measurements of fluorescence resonance energy transfer on cell surfaces. Quantitative evaluation of the transfer efficiency on a cell-by-cell basis. *Biophys. J.* 45: 939-946.
10. Trón, L. 1994. Experimental methods to measure fluorescence resonance energy transfer. In: Mobility and proximity in biological membranes. S Damjanovich, J Szöllősi, L Trón, and M. Edidin, eds. CRC Press, Boca Raton, FL. p 1-47.
11. Szentesi, G., G. Horváth, I. Bori, G. Vámosi, J. Szöllősi, R. Gáspár, S. Damjanovich, A. Jenei, and L. Mátyus. 2004. Computer program for determining fluorescence resonance energy transfer efficiency from flow cytometric data on a cell-by-cell basis. *Comp. Meth. Prog. Biomed.* 75: 201-211.
12. Hanley, Q. S., V. Subramaniam, D. J. Arndt-Jovin, and T. M. Jovin. 2001. Fluorescence lifetime imaging: multi-point calibration, minimum resolvable differences, and artifact suppression. *Cytometry* 43: 248-260.
13. Esposito, A., H. C. Gerritsen, and F. S. Wouters. 2005. Fluorescence lifetime heterogeneity resolution in the frequency domain by lifetime moments analysis. *Biophys. J.* 89: 4286-4299.
14. Murphy, R. M., H. Slayter, P. Schurtenberger, R. A. Chamberlin, C. K. Colton, and M. L. Yarmush. 1988. Size and structure of antigen–antibody complexes. *Biophys. J.* 54:45–56.
15. Kerker, M., M. A. Van Dilla, A. Brunsting, J. P. Kratohvil, P. Hsu, D. S. Wang, J. W. Gray, and R. G. Langlois. 1982. Is the central dogma of flow cytometry true: that fluorescence intensity is proportional to cellular dye content? *Cytometry* 3/2: 71-78.
16. Hirschfeld, T. 1976. Quantum efficiency independence of the time integrated emission from a fluorescent molecule. *Applied optics* 15/12: 3135-3139.

17. Deka, C., B. E. Lehnert, N. M. Lehnert, G. M. Jones, L. A. Sklar, and J. A. Steinkamp. 1996. Analysis of fluorescence lifetime and quenching of FITC-conjugated antibodies on cells by phase-sensitive flow cytometry. *Cytometry* 25: 271-279.
18. MacDonald, R. I. 2006. Characteristics of self-quenching of the fluorescence of lipid-conjugated rhodamine in membranes. *J. Biol. Chem.* 1990; 265/23: 13533-13539.
19. Lakowicz, J. R. 2006. Fluorophores. Ch. 3 *In:* Principles of fluorescence spectroscopy. 3rd ed. Springer p 63-94.
20. Bojarski, C., and K. Sienicki. 1989. Energy transfer and migration in fluorescent solutions. Ch. 1 In: Photochemistry and photophysics, Vol. I. JF Rabek ed., CRC Press, Inc., p 1-56.
21. Bene, L., J. Szöllősi, G. Szentesi, L. Damjanovich, R. Jr. Gáspár, T. A. Waldmann, and S. Damjanovich. 2005. Detection of receptor trimers on the cell surface by flow cytometric fluorescence energy homotransfer measurements. *BBA Mol. Cell Res.* 1744: 176-198.
22. Rényi, A. 1981. Arbitrary random variables. Chapter IV *In:* Probability theory. 4th ed. Tankönyvkiadó, Budapest, p. 161-238.
23. Huber, P. J., and E. M. Ronchetti. 2009. Robust covariance and correlation matrices. Ch. 8. In: Robust statistics. 2nd ed. John Wiley & Sons Inc. p 199-237.
24. Kullback, S. 1997. Properties of information. Ch. 2. In: Information theory and statistics. Dover p 12-31.